Title

Altered metal distribution in the *sr45-1* Arabidopsis mutant causes developmental defects

Short title

Altered Fe homeostasis in *sr45-1*

One sentence summary

The *sr45-1* mutation affects Fe homeostasis, which results in reproductive defects

Authors

Steven Fanara, Marie Schloesser, Marc Hanikenne* and Patrick Motte*

InBioS-PhytoSystems, Functional Genomics and Plant Molecular Imaging and Centre for Assistance in Technology of Microscopy (CAREm), University of Liège, 4000 Liège, Belgium

* Equal contribution

Corresponding authors

Steven Fanara, (steven.fanara@uliege.be; Tel: +32-4-366-38-11)

Correspondence may also be addressed to Marc Hanikenne (marc.hanikenne@uliege.be; Tel: +32-4-366-38-44)

University of Liège

InBioS-PhytoSystems

Quartier de la Vallée, 1

Chemin de la Vallée, 4 - Bât B22

B4000 Liège

Belgium

Author contributions

P.M. and M.H. conceived and directed the research. S.F. conducted most experiments, with contributions of M.S. P.M. and S.F. analyzed most of the data. M.H. and S.F. analyzed the RNA-

Seq data. P.M. and M.H. supervised experiments. S.F. made the figures. S.F., P.M. and M.H. wrote the manuscript, with comments of M.S.

Abstract

The plant SR (serine/arginine-rich) splicing factor SR45 plays important roles in several biological processes, such as splicing, DNA methylation, innate immunity, glucose regulation and ABA signaling. A homozygous Arabidopsis *sr45-1* null mutant is viable, but exhibits diverse phenotypic alterations, including delayed root development, late flowering, shorter siliques with fewer seeds, narrower leaves and petals, and unusual numbers of floral organs. Here, we report that the *sr45-1* mutant presents an unexpected constitutive iron deficiency phenotype characterized by altered metal distribution in the plant. RNA-Sequencing highlighted severe perturbations in metal homeostasis, phenylpropanoid pathway, oxidative stress responses, and reproductive development. Ionomic quantification and histochemical staining revealed strong iron accumulation in the *sr45-1* root tissues accompanied by an iron starvation in aerial parts. We showed that some *sr45-1* developmental abnormalities can be complemented by exogenous iron supply. Our findings provide new insight into the molecular mechanisms governing the phenotypes of the *sr45-1* mutant.

Introduction

The precursor messenger RNA (pre-mRNA) splicing process is a crucial step in the regulation of gene expression. Splice-site selection is carried out by the binding of many *trans*-acting factors including the serine/arginine-rich (SR) splicing factors (Meyer *et al.*, 2015; Jeong, 2017). Alternative splicing (AS) of a specific pre-mRNA can lead to the synthesis of multiple mRNAs and affects up to 70% of multi-exon genes in Arabidopsis (*Arabidopsis thaliana*) (Chamala *et al.*, 2015). AS allows plants to cope with environmental challenges by modulating gene expression and biological processes (Palusa *et al.*, 2007; Palusa and Reddy, 2010; Shang *et al.*, 2017). SR proteins belong to a highly conserved family in multicellular eukaryotes and are characterized by a modular structure consisting of one or two N-terminal RNA-binding domains, called RNA recognition motifs (RRMs), and a C-terminal domain rich in arginine-serine dipeptide repeats (RS) mainly involved in protein-protein interactions (Barta *et al.*, 2010; Manley and Krainer, 2010; Califice *et al.*, 2012). In Arabidopsis, nineteen SR proteins constitute seven subfamilies according to their specific modular organization (Califice *et al.*, 2012). Among these, the atypical SR45 protein contains two RS domains flanking a central and unique RRM (Golovkin and Reddy, 1999). The *sr45-1* null mutant exhibits some developmental defects, including delayed root development, late flowering, shorter siliques with fewer seeds, narrower leaves and petals, and unusual numbers of floral organs (Ali *et al.*, 2007; Zhang *et al.*, 2017). *SR45* undergoes alternative splicing producing two isoforms: the isoform *SR45.1* diverges from *SR45.2* by eight amino acids due to the presence of an additional 21-nucleotides sequence (Zhang and Mount, 2009). These isoforms fulfil distinct roles during Arabidopsis development, since *SR45.1* restores exclusively flowers defect and *SR45.2* only complements the delayed root development when expressed in the *sr45-1* background (Zhang and Mount, 2009).

SR45 was demonstrated to regulate the splicing of functionally diverse targets, thereby acting in ABA signaling and plant defense (Carvalho *et al.*, 2010; Xing *et al.*, 2015; Zhang *et al.*, 2017). SR45 can act as a negative regulator of glucose and ABA signaling during early seedling development by modulation of SnRK1.1 stability through regulation of *5PTase13* splicing under glucose treatment (Carvalho *et al.*, 2010; Carvalho *et al.*, 2016). Knockout mutants for *RS40*, *RS41* and *SR45* all displayed ABA hypersensitivity (Carvalho *et al.*, 2010; Chen *et al.*, 2013). The *sr34b* mutation leads to the stabilization of an alternatively spliced *IRON-REGULATED TRANSPORTER 1* (*IRT1*) mRNA. Accumulation of the IRT1 divalent cation transporter in turn

induces an increased uptake of cadmium (Cd) ions into the root, hence a hypersensitivity to the toxic metal Cd (Zhang *et al.*, 2014). Mutations of several *SR* factors in rice (*Oryza sativa*) also depict the critical role played by alternative splicing in plant response to mineral nutrient status (Dong *et al.*, 2018). Plant SR proteins actively participate to the regulation of alternative splicing under abiotic stress (Laloum *et al.*, 2018; Albaqami *et al.*, 2019).

Iron (Fe) is an essential micronutrient and cofactor responsible for redox state modulation (Nouet *et al.*, 2011; Thomine and Vert, 2013). Since an overproduction of reactive oxygen species (ROS) may result from Fe overaccumulation (Ravet *et al.*, 2009), a physiological balance of Fe uptake and accumulation has to be controlled and maintained in plant. Dicots such as Arabidopsis rely on a three-step reduction-based strategy to acquire Fe (Römheld and Marschner, 1986). The H^+-ATPase AHA2 mediates proton extrusion, which leads to local soil acidification and Fe solubilization (Santi and Schmidt, 2009). With the help of chelators, such as coumarin phenolic compounds (scopoletin, fraxetin and sideretin) that greatly facilitate the acquisition of solubilized Fe from soils (especially at high pH $\geq$ 7) (Mladenka *et al.*, 2010; Fourcroy *et al.*, 2014; Schmidt *et al.*, 2014; Rajniak *et al.*, 2018; Siwinska *et al.*, 2018; Tsai *et al.*, 2018), the enzyme FERRIC REDUCTION OXYDASE 2 (FRO2) catalyzes the reduction of ferric [Fe(III)] to ferrous [Fe(II)] Fe (Robinson *et al.*, 1999). The import of the ferrous Fe ions into root cells is finally performed by IRT1 (Vert *et al.*, 2002; Castaings *et al.*, 2016). Those three major components, as well as transcription factors from the myeloblastosis (MYB) family (MYB10 and MYB72) and several Fe homeostasis genes, are under the positive regulation of the basic helix-loop-helix (bHLH) transcription factor FER-LIKE IRON DEFICIENCY INDUCED TRANSCRIPTION FACTOR (FIT) (Colangelo and Guerinot, 2004; Jakoby *et al.*, 2004; Ivanov *et al.*, 2012; Sivitz *et al.*, 2012). While ETHYLENE INSENSITIVE3 (EIN3) and ETHYLENE INSENSITIVE3-LIKE1 (EIL1) promote its stability upon Fe deficiency (Lingam *et al.*, 2011), ZAT12, BTSL1, BTSL2 and MYC2 target FIT for proteasomal degradation to avoid intake of potentially toxic metals by IRT1 upon prolonged Fe deficiency (Le *et al.*, 2016; Cui *et al.*, 2018; Rodríguez-Celma *et al.*, 2019). Together with its paralog MYB10, MYB72 regulates the expression of two NICOTIANAMINE SYNTHASE, *NAS2* and *NAS4*, in order to facilitate the Fe redistribution in the plant by controlling the biosynthesis of the Fe chelator NA (Palmer *et al.*, 2013). Another bHLH (POPEYE, PYE) is also transcriptionally involved in Fe redistribution, especially through the expression regulation of *NAS4* and *ZIF1*, a vacuolar nicotianamine

transporter (Long *et al.*, 2010; Haydon *et al.*, 2012). A RING E3 ubiquitin ligase, BRUTUS (BTS), compromises the Fe root-to-shoot translocation network controlled by PYE by targeting PYE-interacting transcriptional co-regulator for 26S proteosomal degradation (Kobayashi *et al.*, 2013; Selote *et al.*, 2015; Hindt *et al.*, 2017). The root-to-shoot translocation of Fe involves the loading of citrate and Fe in the xylem respectively by the citrate efflux transporter FERRIC REDUCTASE DEFECTIVE 3 (FRD3) (Durrett *et al.*, 2007) and possibly by Ferroportin 1 (FPN1) (Morrissey *et al.*, 2009). Since endodermis suberization alters the uptake of nutrient, suberization is particularly delayed in plants growing under Fe deficiency (Baxter *et al.*, 2009; Geldner, 2013; Kamiya *et al.*, 2015; Barberon *et al.*, 2016). This response is tightly regulated by the ethylene and ABA stress hormones which are, respectively, suppressor and activator of suberization and thus are positive and negative regulators of the root Fe-uptake, respectively (Barberon *et al.*, 2016).

Alternative splicing is essential to ensure metal tolerance in plants as seen in *sr* rice mutants (Zhang *et al.*, 2014; Dong *et al.*, 2018). A case example is the *ZINC-INDUCED FACILITATOR 2* (*ZIF2*) gene that undergoes intron retention in its 5'UTR to promote zinc tolerance through enhancement of its translation (Remy *et al.*, 2014). Developmental alterations in the *sr45-1* mutant are strikingly similar to phenotypes associated to altered metal homeostasis, such as shorter roots and shorter siliques with fewer seeds as observed in *frd3-7* or *opt3-2* mutants (Stacey *et al.*, 2008; Roschzttardtz *et al.*, 2011). Although many genes involved in root responses to Fe deficiency have been identified, much less is known about the importance of their post-transcriptional processing. In this study, we explored the contribution of SR45 to Fe homeostasis in Arabidopsis roots. We show that the vegetative development of *sr45-1* plants is greatly impacted under Fe deficiency. Upon Fe supply, roots are slightly shorter because of Fe accumulation in the vascular system and the production of an oxidative burst. Fe is less concentrated in the aerial part of the mutant compared to wild-type because of impaired root-to-shoot translocation. We performed RNA-Sequencing (RNA-Seq) on wild-type and *sr45-1* roots upon Fe deficiency and control condition, which demonstrated dramatic transcriptional changes of genes involved in Fe homeostasis, ROS responses and reproductive development. As a consequence, a local metal imbalance appears in reproductive tissues of *sr45-1*, leading to shorter siliques, reduced seed number per silique, and smaller and narrower seeds. These phenotypes are fully restored in mutant plants upon exogenous Fe supply, revealing a connection between Fe

uptake and developmental defects of *sr45-1*.

Results

The "Metal ion transport" GO category is enriched among SR45-associated RNAs

RNA-precipitation experiments recently conducted on seedlings and inflorescences revealed that SR45 binds to and regulates functionally diverse RNAs referred to as SR45-Associated RNAs (SAR) (Xing *et al.*, 2015; Zhang *et al.*, 2017). Here, we submitted a merged set of SAR (7799 genes) to a functional enrichment meta-analysis to identify the putative processes and pathways controlled by SR45 **(Supplemental Table S1)**: 404 Gene Ontology (GO) categories were significantly (p-value < 0.05) enriched among the SR45 targets and consistently illustrated the previously described phenotypes of the *sr45-1* mutant. For instance, the involvement of SR45 in salt tolerance (Albaqami *et al.*, 2019) was reflected in numerous biological processes related to ion transport. Surprisingly, a biological process called "metal ion transport" (116 genes) was significantly enriched, within which several sub-GO enrichments related to divalent cation and iron transport were further observed **(Supplemental Table S1)**. Moreover, 38.5% of SAR corresponded to genes identified in transcriptomic studies as differentially expressed upon varying Fe supply (hereinafter referred as "iron-responsive genes") **(Supplemental Figure S1)**.

Metal levels are increased in the roots of *sr45-1*

These observations led us to examine whether the *sr45-1* mutation results in any Fe homeostasis perturbation and therefore the ionome was profiled in tissues of both *sr45-1* and WT (Col-0) plants grown in Fe-deficient (0 µM) and Fe-sufficient (10 µM) conditions. In Fe-sufficient condition, the roots of *sr45-1* accumulated more Fe (136%), Mn (218%) and Zn (150%) compared to the WT. In contrast, Cu levels were similar in the two genotypes **(Figure 1A-D)**. Upon Fe deficiency, Fe and Zn accumulated similarly in *sr45-1* and WT roots, but *sr45-1* roots accumulated more Cu (125%) and Mn (146%). Conversely, *sr45-1* accumulated less Fe (52%), Mn (38%), Zn (37%) and Cu (33%) than the WT in shoots under Fe deficiency **(Supplemental Figure S2A-D)**. Accumulation reduction of Fe (17%), Mn (18%) and Zn (32%) was also significant in *sr45-1* shoots under Fe-sufficient condition **(Supplemental Figure S2A and C-D)**. While root macronutrients (Ca, K and Mg) levels were similar between genotypes

under Fe deficiency and sufficiency, Ca levels were reduced by 26% in mutant shoots at 0 µM Fe but K levels were increased by 36% at 10 µM Fe, and no significant changes were observed in mutant shoots regarding Mg levels **(Supplemental Figure S3A-C)**.

In Fe sufficiency condition, Perls' staining revealed strong Fe accumulation in the vascular cylinder of *sr45-1* roots, **(Figure 1E)**, a phenotype strikingly similar to a *ferric reductase defective3* (*frd3*) loss-of-function mutant (Green and Rogers, 2004; Roschzttardtz *et al.*, 2009; Scheepers *et al.*, 2020). Because of this phenotypic similarity, we decided to concomitantly analyse *frd3-7* as a control for defective Fe homeostasis **(Figure 1E)**. No Fe accumulation in root vascular tissues occurred upon Fe deficiency in the three genotypes. It is well described that overaccumulation of Fe can trigger ROS overproduction, ultimately leading to oxidative stress (Reyt *et al.*, 2015). Fe and ROS accumulation were shown to correlate in root vascular tissues of *frd3-7* (Scheepers *et al.*, 2020). DAB staining, revealing H_2O_2 accumulation, was accordingly detected in the central vasculature of the root in both *sr45-1* and *frd3-7* mutants but not in the WT **(Figure 1F)**. Altogether, the Fe accumulation pattern in roots and shoots of *sr45-1* plants are indicative of a defective metal root-to-shoot translocation of Fe in *sr45-1*.

The *sr45-1* mutant is sensitive to the Fe status

Based on these observations, we investigated the effect of Fe supply on the *sr45-1* mutant development by growing either seedlings for 14 days on Fe-depleted (0 µM Fe), control (10 µM Fe) or supplemented with Fe excess (50 µM Fe) agar solid Hoagland or 6-week-old plants in hydroponic solution in Fe-deficient and Fe-sufficient conditions **(Figure 2**, **Supplemental Figure S4A)**. In seedlings, the root growth of the *sr45-1* mutant was reduced by 47% under Fe deficiency and 68% under Fe excess compared to WT **(Supplemental Figure S4A)**. The reduction of root biomass correlated with a reduction of shoot biomass with a loss of 46%, 38.5% and 21% at Fe deficiency, sufficiency and excess, respectively, compared to WT at Fe sufficiency **(Supplemental Figure S4B)**.

In adult plants, *sr45-1* root growth was significantly decreased in both deficiency and excess conditions (**Supplemental Figure S4C**). In response to Fe deficiency, roots of the WT and *sr45-1* were 27.5% and 43% shorter, respectively, compared to Fe sufficiency. Similarly, the shoot fresh weight of both wild-type and *sr45-1* mutant plants was affected by Fe deficiency with a significant biomass loss of 61.5% and 71.3%, respectively, compared to the Fe-sufficient

condition **(Supplemental Figure S4D)**. Although *sr45-1* development was already delayed in control condition, the *sr45-1*/WT ratio for both root length **(Figure 2C)** and shoot fresh weight **(Figure 2D)** indicated that adult *sr45-1* plants were more sensitive to Fe deficiency than the WT. Fe deficiency resulted in chlorosis in shoots of both WT and mutant. However, the aerial parts of the *sr45-1* mutant presented a more severe chlorosis **(Figure 2A-B)** at 0 µM Fe than the WT, confirming higher sensitivity of the mutant to Fe deficiency. Exposure to higher Fe supply (50 µM) additionally suggested that the mutant had a perturbed root-to-shoot Fe translocation: whereas the WT suffered of Fe toxicity with less biomass production in aerial parts in these conditions (significant loss of 34%), higher Fe supply did not cause further delay nor improved shoot growth of adult *sr45-1* plants **(Supplemental Figure S4D)**. This confirmed the impaired Fe root-to-shoot distribution and inferred that increasing Fe supply would trigger toxicity in *sr45-1* roots.

Zinc accumulation in roots of *sr45-1* is toxic

The 2-fold and 1.5-fold increases in accumulation of respectively Mn and Zn in *sr45-1* roots upon Fe sufficiency **(Figure 1C-D)** may cause growth reduction as previously observed (Dučić and Polle, 2007; Lei *et al.*, 2007; Kawachi *et al.*, 2009; Fukao *et al.*, 2011; Shanmugam *et al.*, 2011; Marschner and Marschner, 2012; Millaleo *et al.*, 2013; Scheepers *et al.*, 2020). Thus, we investigated the influence of those metals on the growth of *sr45-1*. Contrary to Mn depletion, Zn depletion did not significantly impact the root growth of the WT in our growth condition on agar plates. In contrast, root length of *sr45-1* was significantly longer by 12% upon Zn deficiency, but roots remained 50% smaller compared to WT in control condition (**Figure 3**), suggesting that Zn accumulation in roots was toxic and indeed partially contributed to the growth defect of *sr45-1*. Mn and Zn deficiency did not influence Fe or H_2O_2 accumulation in the *sr45-1* root vasculature **(Supplemental Figure S5A-B)**.

The shoot fresh weight of *sr45-1*, which was lower by 28% in control condition compared to the WT, was increasingly affected by Mn and Zn deficiencies, leading to a biomass loss of 70% and 73.5%, respectively, compared to the WT in Fe sufficiency **(Supplemental Figure S5C)**. In Zn-deficient condition, Col-0 shoot biomass was decreased by 68.5%, resulting in the absence of significant changes between both genotypes. Altogether, these results pointed to a Zn

toxicity in roots and to a defective metal homeostasis, possibly in acquisition and mobilization of metals.

Transcriptome profiling of *sr45-1* mutant roots

To uncover the molecular mechanisms underlying metal distribution in *sr45-1*, a transcriptomic profiling of WT and *sr45-1* root tissues of adult plants grown hydroponically in Fe-deficient (0 µM) and Fe-sufficient (10 µM) conditions was conducted using RNA-Seq. A limited number of differentially expressed genes (DEGs) [fold change ≥ 2 or ≤ -2 and false discovery rate (FDR) < 0.05] were identified between WT and mutant roots in Fe-sufficient (29 DEGs) and Fe-deficient conditions (49 DEGs) **(Figure 4 and Supplemental Table S2)** and no enriched GO functional category was identified among either of those sets of DEGs **(Supplemental Table S3)**. *sr45-1* mutant plants presented less transcriptomic changes in response to Fe deficiency than Col-0 (1350 *vs* 2442 DEGs) and accordingly, the number of enriched GO biological processes was considerably reduced in the mutant (33 *vs* 50 and 20 *vs* 75 for the up- and down-regulated genes, respectively) **(Supplemental Table S3)**. In fact, in response to Fe deficiency, Col-0 displayed extensive changes in the expression of genes contributing to diverse biological processes that were not over-represented in the mutant roots. For instance, the response of Col-0 roots to Fe deficiency involved the induction of metal ion homeostasis and transport, as well as the repression of several functions including phenylpropanoid biosynthetic process, cell wall modifications, lignin biosynthesis, biotic and hormonal responses **(Supplemental Table S3)**. The molecular alteration in the *sr45-1* mutant roots under Fe deficiency included perturbation in cellular iron ion homeostasis (*FER* and *VTL* genes) and oxidative stress response (through down-regulation of, respectively, 7 and 35 genes), as well as in anion transport and sulfate transport (through up-regulation of, respectively, 34 and 6 genes). Surprisingly, while response to ethylene was a significant over-represented function in both Col-0 and *sr45-1* roots upon Fe deficiency, divergence appeared: 42 genes were under-expressed in Col-0 (against 9 of them in *sr45-1*) and 22 genes were over-expressed in the mutant (against 18 of them in Col-0) **(Supplemental Table S3)**.

To further characterize *sr45-1* root transcriptome and fine-tune our understanding of the metal homeostasis regulated by SR45, additional comparisons were performed to discover SR45 differentially regulated genes (SDR; DEGs significantly and specifically deregulated in *sr45-1*

roots in respective comparison) **(Figure 4)**: SDR included 304 and 387 in the comparison of the Fe deficiency DEGs in the WT (2442 genes) with either (i) the Fe deficiency DEGs in the mutant (1350 genes) or (ii) the DEGs between mutant at Fe deficiency and the WT in control condition (2000 genes), respectively. The reciprocal of the latest comparison yielded 259 additional SDR. Finally, 827 SDR were obtained when intersecting the DEGs obtained when comparing a genotype (WT or *sr45-1*) in deficiency with the other genotype in sufficiency. Together with the DEGs identified between genotypes in Fe-sufficient (29) and Fe-deficient (49) conditions, it represented 1071 unique SDR compared to 1844 CDR (Col-0 differentially regulated genes) **(Supplemental Table S4)**. The analysis of GO enrichment highlighted molecular contribution of both CDRs and SDRs to many similar biological pathways. However, CDRs included genes involved in biological functions that were not over-represented in the mutant, such as response to jasmonic acid and ethylene, cell wall organization, phenylpropanoid biosynthetic and metabolic processes or lignin metabolic process **(Figure 4B**, **Supplemental Table S5)**. SDRs contribute additionally to two biological functions unrepresented in CDRs, namely chemical homeostasis and response to organonitrogen compound, which include genes involved in Fe, Mn, Zn, Cu and Cd homeostasis **(Figure 4C**, **Supplemental Table S5)**.

These observations gave evidence that the mutant is pervasively affected in many pathways upon Fe deficiency. It raised the question whether *sr45-1* mutant plants were able to accurately regulate the response of key genes or whether adult mutant plants were coping with residual induction of the metal homeostasis due to defective seedlings (as shown by the severe toxic symptoms displayed in response to Fe supply **(Supplemental Figure S4)**.

The Fe acquisition machinery is constitutively induced in *sr45-1* seedlings

As the ionome and the growth of the mutant were affected by the Fe status (**Figure 1** and **Supplemental Figure S4**), gene expression (using qRT-PCR) and protein activity of key components of the Fe uptake machinery were examined in roots of 14-day-old seedlings, as well as 9-week-old roots grown in Fe deficiency and sufficiency conditions. The expression of the bHLH transcription factor *FIT* was up-regulated by Fe deficiency in both WT and *sr45-1* seedling roots compared to the 10 µM Fe condition. However, *FIT* expression was ~47-51% higher in *sr45-1* seedlings compared to Col-0 in both Fe-sufficient and Fe-deficient conditions **(Figure 5A)**. Similarly, the FIT targets *AHA2*, *FRO2* and *IRT1* were also more highly expressed

(124-208%) in *sr45-1* roots in both conditions compared to Col-0 **(Figure 5B-D)**, consistent with increased acidification of the medium (mostly driven by AHA2) **(Supplemental Figure S6A)** and ferric chelate reductase activity (mostly driven by FRO2) in *sr45-1* roots **(Supplemental Figure S6B)**. Altogether, these observations were indicative of a constitutive Fe deficiency response in *sr45-1* roots upon control Fe supply (10 µM). This response was further aggravated when no Fe (0 µM) was supplied.

In adult roots, all key components of the Fe uptake machinery were induced in both Col-0 and *sr45-1* upon Fe deficiency, but no significant deviation was observed between genotypes for *FIT*, *FRO2* or *IRT1* expression. However, *AHA2* expression was ~36.8% higher in *sr45-1* roots compared to Col-0. While *FIT* expression was not induced in adult mutant roots at Fe deficiency or sufficiency **(Figure 5A)**, the expression of genes encoding the MYB72, bHLH38, bHLH39, bHLH100 and bHLH101 transcription factors, which are known to act in conjunction with FIT to induce the Fe acquisition machinery (*AHA2*, *FRO2* and *IRT1*) (Yuan *et al.*, 2008; Palmer *et al.*, 2013; Wang *et al.*, 2013), was significantly up-regulated in the *sr45-1* mutant under Fe deficiency compared to Col-0 **(Supplemental Figure S7)**.

Since Fe accumulation in the root vasculature was observed in both *sr45-1* and *frd3-7* mutants, the relative expression level of *FRD3* in *sr45-1* roots was also analyzed. The level of *FRD3* was reduced by 29% and 25% in the mutant upon Fe-deficient and Fe-sufficient conditions, respectively **(Figure 5E)**. In agreement with this observation, both *sr45-1* and *frd3-7* accumulated a higher level of citrate, the substrate of FRD3, in roots, but it was significantly lower in *sr45-1* **(Supplemental Figure S6C)**. In contrast, adult mutant roots did not show any deviation in *FRD3* expression compared to the WT **(Figure 5E)**.

All results suggested that, contrary to adult plants, *sr45-1* seedlings display a constitutive iron deficiency response independently of the iron concentration used (0 µM or 10 µM Fe) and that the root-to-shoot Fe translocation may be impaired through down-regulation of *FRD3* in young roots.

Influence of coumarins on the developmental defects of *sr45-1* mutant seedlings

The phenylpropanoid pathway, which participates in the synthesis of coumarins involved in Fe solubilization from the soil, including through a transcriptional control by BEE1 and MYB15 (Petridis *et al.*, 2016; Chezem *et al.*, 2017), both identified as SDR in this study, is improperly

regulated in *sr45-1* adult roots **(Supplemental Table S3** and **Supplemental Table S5)**. In fact, many genes were down-regulated in Col-0 in response to Fe deficiency, but only few of them were affected in this fashion in the mutant **(Supplemental Figure S8)**. This suggested that Fe mobilization from the soil may be affected in the mutant. To investigate this hypothesis, Col-0 and mutant seedlings were grown on solid Hoagland media containing or not Fe-mobilizing compounds and supplemented with 10 µM Fe. A Hoagland control medium, containing Fe-HBED at pH 5.7, was used as the maximum of Fe bioavailability, and a Hoagland unavailable Fe medium, containing $FeCl_3$ at neutral pH, was used as the minimum of Fe bioavailability (Tsai *et al.*, 2018). Whereas the root growth of the WT was significantly reduced (~10%) on $FeCl_3$ medium, it was increased by ~29% in the mutant **(Figure 6A)**, which confirms that Fe in a soluble form causes toxicity in *sr45-1* roots. No signal of iron accumulation nor oxidative stress was visualized in seedlings grown on the unavailable Fe medium **(Figure 6B-C)**. This suggested that *sr45-1* is less capable of mobilizing Fe from the Fe unavailable medium. We then tested whether supplementation of coumarins could help the mutant in this regard. Exogenous application of fraxetin did not affect the root growth of Col-0 nor *sr45-1* **(Figure 6A)** but led to an increase in the Fe and H_2O_2 accumulation in the mutant roots compared to the $FeCl_3$ only condition **(Figure 6B-C)**. In the absence of Fe (0 µM $FeCl_3$), no significant change in the length of WT roots was observed, but the mutant roots were significantly longer by 8.5% compared to the Fe unavailable condition, further indicating the Fe toxicity in the mutant. The further addition of fraxetin led to a significant decrease of both Col-0 (~13.5%) and *sr45-1* (~12.5%) root length **(Figure 6A),** whereas no Fe nor H_2O_2 staining was observed in seedlings **(Figure 6B-C)**. This suggests that coumarins tend to mobilize Fe (and possibly other metals) from the medium, which restores metal toxicity in the mutant.

In presence of unavailable Fe, the shoot fresh weight of Col-0 or *sr45-1* were significantly reduced by ~33% and ~5.5% compared to themselves in control condition **(Supplemental Figure S9A-B)**, confirming that the mutant shoots initially suffered of an iron deficiency that was not significantly aggravated in presence of unavailable Fe. Supplementation of coumarins affected the shoot fresh weight of the seedlings in the same fashion than the unavailability of Fe **(Supplemental Figure S9A-B)**, which suggests that despite the improved solubilization and uptake of Fe, the mutant did not efficiently translocate Fe from roots to shoots to ensure proper

development. The total chlorophyll content of the WT or the mutant was not significantly affected in any of the tested conditions **(Supplemental Figure S9C)**.

Although the phenylpropanoid pathway is deregulated, the function of fraxetin is not defective in the mutant. In fact, the mutant is capable of remobilizing iron from the insoluble $FeCl_3$ salt in presence of this coumarin, leading to root iron accumulation but not toxicity.

Iron supplementation fully restored all the reproductive phenotypes of *sr45-1* mutant plants

We last questioned if the *sr45-1* phenotypes of shorter siliques and reduction in seed yield (Zhang *et al.*, 2017) could be rescued by Fe supplementation, as shown for the *frd3-7* mutant (Roschzttardtz *et al.*, 2011). Col-0 and *sr45-1* plants were therefore grown on soil until seed setting. They were daily irrigated with water without (–Fe) or with an additional treatment consisting of a weekly irrigation with sequestrene (+Fe). The sequestrene irrigation of the soil fully restored silique length **(Figure 7A-B)** and seed number per silique in the *sr45-1* mutant **(Figure 7D)**. The "shrunken" phenotype of the *sr45-1* seeds compared to Col-0, consisting of a decreased seed length, width and mass, was also fully restored upon Fe irrigation **(Figure 7C and 7E-F)**. However, Fe-irrigated mutants still displayed impaired growth of stem **(Supplemental Figure S10A)** and late flowering upon Fe treatment **(Supplemental Figure S10B-C)** (Ali *et al.*, 2007). This suggested that the complementation by Fe was specific to seed development.

To examine whether defects in seed morphology were linked to perturbed metal concentrations, an ionomic analysis was conducted on –Fe and +Fe seeds. Compared to WT seeds, *sr45-1* seeds displayed significantly increased in Zn, K and Mg levels but contained reduced amount of Mn. Upon Fe irrigation, these defects were completely restored for all metals but Mn **(Figure 7G-J)**. In the case of Zn, the Fe supplementation did not modulate the Zn concentration in mutant seeds but increased the Zn concentration in the one of Col-0 **(Figure 7G)**. Finally, no defect was detected in mutant seeds for micronutrients Fe and Cu, nor macronutrients Ca and P **(Supplemental Figure S10D-G)**, but Fe irrigation increased the Cu content in both WT and *sr45-1* seeds **(Supplemental Figure S10E)**. Altogether, these results suggested that the mutant seeds contained abnormal concentrations of metals and that Fe supplementation was able to restore all the ion defects (but Mn) in the mutant seeds.

Discussion

SR45, an atypical SR protein containing two RS domains, is an auxiliary component of the spliceosome whose biological functions remained elusive (Califice *et al.*, 2012). It has been recently shown that this splicing factor regulates diverse biological processes including abscisic acid signaling and innate immunity, thanks to the identification of its direct targets (SARs) in two complementary studies (Xing *et al.*, 2015; Zhang *et al.*, 2017). Here, combining these two datasets, identifying SARs (7799) (Xing *et al.*, 2015; Zhang *et al.*, 2017) and SDR genes (358) in reproductive tissues (Zhang *et al.*, 2017), with an RNA-Seq analysis of the roots of the *sr45-1* mutant upon changes in Fe supply, identifying 1071 SDR genes, allowed to better describe major defects linked to the *sr45-1* mutation and hence to better depict a global function of SR45. Eighteen genes emerged as shared among SARs and SDR genes, representing probable SR45 RNA targets that are constantly deregulated regardless of the tissue and stage of development of the *sr45-1* mutant (e.g. *MYB15*, *PWD/GWD2*, *OCT3* or *AtHMP37*) **(Supplemental Table S6)**. Loss-of-function mutants of several SDR genes identified in this study display abnormal silique length and seed set, as well as seed abortion **(Supplemental Table S5 and Supplemental Figure S11)**, which are also strong phenotypes of the *sr45-1* mutant (Zhang *et al.*, 2017). Among these knock-out lines, the mutation of *PWD/GWD2* (*AT4G24450*) leads to a reduced number of siliques and a decreased seed production, and *pwd/gwd2* seeds are shrunken with an irregularly shaped coat (Pirone *et al.*, 2017). The *PWD/GWD2* gene is not only a putative target of SR45 splicing activity (SAR) but was also identified in a set of 918 differentially expressed genes in *sr45-1* seedlings (Xing *et al.*, 2015) and as down-regulated in roots of adult *sr45-1* plants here. Even though several phenotypes, including reduced growth rate of the primary root (Pirone *et al.*, 2017), of the *pwd/gwd2* mutant are a surprising reminiscence of the root and reproductive defects we observed in *sr45-1* **(Figure 2** and **Figure 7)**, it was recently shown that the down-regulation of *PWD/GWD2* expression does not correlate with a protein decrease in the *sr45-1* mutant inflorescences (Chen *et al.*, 2019). However, because the PWD/GWD2 function is restricted to the companion cells (Glaring *et al.*, 2007) and consists in sustaining the phloem loading of polysaccharides in source organs (Pirone *et al.*, 2017), the absence of protein accumulation changes in inflorescences is not relevant in regards to the primary root cellular function played by this protein (Pirone *et al.*, 2017). Therefore, the reproductive defects of *sr45-1* might not be solely associated to the down-regulation of *PWD/GWD2*, which is confirmed by the fact that Fe

supplementation is able to rescue the reproductive defects of the mutant **(Figure 8)** in the absence of regulation of *PWD/GWD2* **(Supplemental Figure S11)**. These results strongly suggest that part of the silique and seed developmental defects is related to altered metal homeostasis in reproductive organs, which is known to tremendously affect anther dehiscence, pollen development, fruit development, seed quality and seed yield (Verbruggen and Hermans, 2013; Guo *et al.*, 2016; Singh and Reddy, 2017).

Supporting this hypothesis, *sr45-1* mutant seeds contain decreased amounts of Mn as well as increased levels of macronutrients K, Mg and Zn, possibly accounting for the reproductive defects upon water irrigation, i.e. in the absence of Fe supplementation **(Figure 7)**. Previously, the expression of several ion transporter-encoding genes was shown to be deregulated in *sr45-1* inflorescences (Zhang *et al.*, 2017). Indeed, *AtHMP37* (*AT4G27590*) and *AtHMP27* (*AT3G24450*), *PCR2* and *HIPP22*, respectively encoding two heavy metal transport/detoxification superfamily proteins (Li *et al.*, 2020), a zinc transporter (Song *et al.*, 2010) and a cadmium-detoxifying protein (Tehseen *et al.*, 2010), are all up-regulated in *sr45-1* inflorescences (Zhang *et al.*, 2017). The member of the heavy metal transport/detoxification superfamily, *AtHMP37*, is a SDR gene (in both roots and inflorescences) identified as a putative RNA target of SR45 (SAR) **(Supplemental Table S6)** (Xing *et al.*, 2015; Zhang *et al.*, 2017) that is up-regulated in *sr45-1* roots **(Supplemental Figure S13)**. On the contrary, the *NFP7.1* gene, which encodes a nitrate transporter (Babst *et al.*, 2019), and the NRT1.7 nitrate transporter (Fan *et al.*, 2009; Liu *et al.*, 2017b), were shown to be down-regulated in *sr45-1* inflorescences (Chen *et al.*, 2019). It is well known that the N status affects Mg and Fe homeostasis (e.g. *FIT* regulation) (García *et al.*, 2010; Curie and Mari, 2017; Liu *et al.*, 2017a; Kailasam *et al.*, 2018; Liu *et al.*, 2018) and that a crosstalk exists between Zn and Fe homeostasis through at least IRT1, ZIF1 and FRD3 (Haydon *et al.*, 2012; Charlier *et al.*, 2015; Scheepers *et al.*, 2020; Hanikenne *et al.*, 2021). It is therefore possible that changes in the levels of micro- and macronutrients in seeds are the result of deregulation in the expression of nutrient transporters or *vice versa*, the causality between these observations being difficult to determine from our data. In fact, the mutant root growth is altered by Fe supply from the first week of development **(**see **Supplemental Figure S12)** and continues to be drastically affected upon extensive exposure **(Figure 2)**.

Surprisingly, while Fe concentration was diminished in the *sr45-1* mutant shoots upon both Fe deficiency and sufficiency **(Supplemental Figure S2)**, it is very similar in seeds of Col-0

and *sr45-1* **(Supplemental Figure S10D)**. This suggest that the cause of the *sr45-1* developmental defects in reproductive organs is not Fe starvation of the embryo but rather a consequence of intricate ionome perturbations. In fact, Zn concentration in seeds obtained from plants watered with solely tap water was higher (84.5 %) in the mutant compared to the WT, suggesting that the radicle local environment contained a higher Zn pool, which may result in a local Fe deficiency as previously observed (Dučić and Polle, 2007; Lei *et al.*, 2007; Kawachi *et al.*, 2009; Fukao *et al.*, 2011; Shanmugam *et al.*, 2011; Marschner and Marschner, 2012; Millaleo *et al.*, 2013; Scheepers *et al.*, 2020). The constitutive induction of the Fe uptake machinery **(Figure 5)** in the *sr45-1* seedlings would reflect this ionome and possibly Fe defect in the seeds. However, the primary root growth of seeds collected from *sr45-1* plants supplemented with Fe was not significantly improved compared to seeds collected from plants watered with tap water **(Supplemental Figure S12)**. It is therefore still unclear how altered partitioning of metals in the mutant seeds affects the primary growth of the seedling.

It is however evident that *sr45-1* seedlings and plants exhibit several alterations of metal homeostasis: (i) Fe and H_2O_2 accumulation within the root vasculature; (ii) Mn and Zn accumulation in roots and (iii) reduced shoot metal (Fe, Zn, Mn) concentrations, resulting in reduced biomass and chlorosis upon changes in Fe supply. RNA-Seq and qRT-PCR analyses suggest that mutant roots displayed a basal induction of Fe-starvation-responsive genes in control conditions with less drastic expression changes compared to Col-0 upon Fe deficiency (1350 *vs* 2442 DEGs) in adult plants **(Figure 4, Supplemental Figures S7 and S13)** and a stronger response in seedlings (**Figure 5, Supplemental Figure S6**).

Our working hypothesis therefore stands in favor of a scenario where the defective seed ionome affects the development of the embryo, which consequently results in an induction of the Fe uptake machinery in seedlings upon germination **(Figure 5A-D)** in an attempt to compensate for the metal starvation **(Figure 7J)**. The down-regulation of *FRD3* expression in seedlings **(Figure 5E)** would reduce root-to-shoot translocation of citrate-complexed metals that may reveal toxic when in excess in aerial parts (i.e. Fe, Zn). This ultimately results in lower shoot biomass and metal concentrations **(Figure 1 and Supplemental Figure S2)**, together with Fe and Zn toxicity in roots **(Figure 3)**, including the accumulation of H_2O_2 **(Figure 1F** and **Supplemental Figure S5B)**. If ionome and growth perturbations persist in mutant adult plants

(Figure 7G-J), their effect on Fe and metal homeostasis gene expression appear mitigated **(Figure 4** and **Figure 5)**.

Conclusion

We reported here that some of the *sr45-1* mutant phenotype result from a severe alteration in metal mobilization, localization and transport. We also showed that exogenous application of Fe can rescue the reproductive defects of the mutant. Our data fine-tune our understanding of the physiological responses impaired in the mutant, such as the oxidative response, metal homeostasis and the phenylpropanoid pathway.

Methods

Plant material and growth conditions

All experiments were conducted under a 8-h-light (100 µmol m^{-2} s^{-1})/16-h-dark regime in a climate-controlled growth chamber (21°C). *Arabidopsis thaliana* ecotype Columbia-0 (Col-0) was used as wild-type, and seeds from *sr45-1* mutant (SALK_004132, Col-0 background) and *frd3-7* mutant (SALK_122235, Col-0 background) were obtained from the SALK collection. Seeds were surface-sterilized and germinated on 1/2 Murashige and Skoog (MS) medium (Duchefa Biochimie) supplemented with sucrose (1% w/v, Duchefa Biochimie) and Select Agar (0.8% w/v, Sigma-Aldrich) and stratified in the dark at 4°C for 48h. For hydroponics experiments, 3-week-old seedlings were transferred in hydroponic trays (Araponics) and cultivated for 3 weeks in control Hoagland medium, followed by 3 weeks of experimental conditions. The nutrient medium was renewed with fresh solution once a week and 3 days prior to the harvesting. The control Hoagland medium included 10 µM FeIII-HBED [N,N'-di(2-hydroxybenzyl) ethylenediamine N,N'-diacetic acid monohydrochloride], 1 µM Zn ($ZnSO_4.H_2O$) and 5 µM Mn ($MnSO_4.H_2O$) as reported in (Talke *et al.*, 2006; Hanikenne *et al.*, 2008; Scheepers *et al.*, 2020). Fe, Zn and Mn were respectively added or omitted from medium as described.

Unless stated otherwise, for root length measurement (including treatments with 120 µM of DMF-solubilized fraxetin), Perls and hydrogen peroxide staining, acidification capacity assay, FeIII chelate reductase activity assay and citrate content measurement, surface-sterilized seeds were directly sown on square plastic Petri plates (Greiner Bio-One) containing modified

Hoagland supplemented with sucrose (1% w/v, Duchefa Biochimie), FeIII-HBED (0 µM to 50 µM) and agar (0.8% w/v, Agar Type M, Sigma-Aldrich), and grown vertically after stratification.

Seed number per silique, seed morphology, silique size and roots length

3-weeks-old seedlings were transferred in soil and daily watered with water (referred to as –Fe). In addition of this treatment, half of the seedlings from each genotype were weekly supplied with a sequestrene solution (referred to as +Fe, 0.1 g/L, Liro N.V.) until the completion of silique development and seed maturation. Siliques were then harvested before dehiscence, and their size was determined using the segmented line tool on ImageJ. After an incubation of two weeks in 95% ethanol at room temperature, the seed number per silique was determined under a Nikon SMZ1500 stereomicroscope. Seeds were finally photographed using a Nikon SMZ1500 stereomicroscope equipped with a Nikon Digital Sight DS-5M camera in order to determine seed length and width.

Perls and hydrogen peroxide staining

For Perls staining, roots of *Arabidopsis thaliana* Col-0 and *sr45-1* mutant seedlings (or 9-week-old plants) were vacuum infiltrated with HCl (4%, v/v) and K-Ferrocyanide (II) (4%, w/v, Sigma-Aldrich) (1/1) for 15 minutes. The reaction was continued for an additional 30 minutes at room temperature and was then stopped by substituting the solution by distilled water (Roschzttardtz *et al.*, 2009). Observation was realized using a Nikon SMZ1500 stereomicroscope equipped with a Nikon Digital Sight DS-5M camera.

Hydrogen peroxide (H_2O_2) was detected according to (Baliardini *et al.*, 2015). Roots samples were vacuum infiltrated with 3-3'-diaminobenzidine tetrahydrochloride (1.25 mg/mL, DAB, Sigma-Aldrich), Tween-20 (0.05% v/v) and 200 mM Na_2HPO_4, then incubated in the same solution for a total of one hour. They were subsequently bleached in acetic-acid/glycerol/ethanol (1/1/3) during 5 minutes at 100°C, and stored in glycerol/ethanol (1/4) before further analysis. Samples were observed under a stereomicroscope as above.

Acidification capacity and Ferric (FeIII) chelate reductase activity assays

For the measure of acidification capacity, roots from a pool of 5 seedlings were incubated in 0.005% bromocresol purple (Roth) during 24 hours in the dark. A_{433} of the protonated form of

the dye was then measured and expressed relative to the root weight of sample (Santi and Schmidt, 2009; El-Ashgar *et al.*, 2012).

The ferric chelate reductase (FCR) activity was measured on roots from a pool of 5 seedlings. Samples were immerged in a reductase solution containing FeIII-EDTA (0.1 mM, Roth) and FerroZine (0.3 mM, Acros Organics) for 30 minutes in the dark. A_{562} of the FeII-FerroZine complex was then determined. The final calculation included the root weight of sample and the molar extinction coefficient of the complex (28.6 $mM^{-1}.cm^{-1}$) (Yi and Guerinot, 1996).

Citrate content

Citrate determination was performed as previously described (Schvartzman *et al.*, 2018). Briefly, 100 mg of roots were frozen and grinded in liquid nitrogen with a mortar and pestle. Samples were resuspended in 1 mL of distilled water, and the pH was adjusted to 7 – 8 with 1 M KOH. Samples were deproteinized using 100 µL of 1 M perchloric acid, and citrate content was measured using a citric acid assay kit according to the manufacturer's protocol (BioSentec, France).

Total chlorophyll and carotenoid content

Total chlorophyll content was determined from three to six young seedlings or the rosette of one 9-week-old plant. Plants were weighed, then incubated in the dark during 72h or seven days in 95% ethanol. Discolored plants were removed and the solution was submitted to spectroscopic analysis. The total amount of chlorophyll was calculated using the equation: $\text{Chl } a + b = \frac{6.1\ A_{665} + 20.04\ A_{649}}{\text{fresh weight}}$ (Wintermans and de Mots, 1965). Carotenoid content (xanthophylls and carotenes) was determined for the same samples using the equation: $\text{C(x + c)} = \frac{\frac{1000\ A_{470} - 2.13\ \text{Chl } a - 97.64\ \text{Chl } b}{209}}{\text{fresh weight}}$ (Lichtenthaler and Buschmann, 2001).

Gene expression analysis

Total RNAs were extracted from 100 mg of plant tissues (entire plants or roots) using NucleoSpin RNA Plant kit (Macherey Nagel) as per manufacturer's instruction. cDNAs were synthesized from 1 µg of total RNAs using oligo(dT) and the RevertAid H Minus First Strand cDNA Synthesis Kit (Fisher Scientific). Quantitative PCR reactions were performed in a

QuantStudio5 (Applied Biosystems) using 384-well plates and Takyon Low Rox SYBR MasterMix dTTP Blue (Eurogentec) on material from three independent biological experiments, and a total of three technical repeats were run for each combination of cDNA and primer pair. Gene expression was normalized relative to At1g58050 as described (Pfaffl, 2001). *At1g58050* expression was the more stable among all tested references (*EF1α* and *UBQ10*) (Czechowski *et al.*, 2005; Spielmann *et al.*, 2020). **Supplemental Table S7** shows the primers used for these experiments.

Upon harvesting, plant root tissues were blotted dry, immediately frozen in liquid nitrogen and stored at -80°C. Total RNAs were prepared using 100 mg of homogenized tissues and RNeasy Plant Mini kit with on-column DNase treatment (Qiagen). Libraries for RNA-Seq were prepared from 1 µg of total RNAs with the TruSeq Stranded mRNA Library Prep Kit (Illumina, CA, USA), multiplexed and sequenced in two runs with an Illumina NextSeq500 device (high throughput mode, 75 base single-end reads) at the GIGA-R Sequencing platform (University of Liège), yielding on average ~22 million reads per sample. Read quality was assessed using FastQC (v0.10.1, http://www.bioinformatics.babraham.ac.uk/projects/fastqc/). Quality trimming and removal of adapters were conducted using Trimmomatic (v0.32, Bolger *et al.*, 2014), with the following parameters: trim bases with quality score lower than Q26 in 5' and 3' of reads; remove any reads with Q<26 in any sliding window of 10 bases; crop 1 base in 3' of all reads, and discard reads shorter than 70 bases. Overall quality filtering discarded between 7 and 9% of the raw reads. The Arabidopsis reference genome sequence (TAIR10) and annotation (201606 version) files were downloaded from Araport on Sept 16, 2016 (www.araport.org). Read mapping on the genome was achieved using TopHat (v2.1.1), with the following parameters: --read-mismatches 2; --min-intron-length 40; --max-intron-length 2000; 2 --report-secondary-alignments; --no-novel-juncs and providing an indexed genome annotation file. Raw read counts were obtained using htseq-count (v0.6.1p1) and differentially expressed genes were identified by pairwise comparisons with the DESeq2 package (v1.12.3, Love *et al.*, 2014). Genes were retained as differentially expressed when the $\log_2$ fold-change (FC) was > 1 or < -1, with a false discovery rate (FDR, Benjamini-Hochberg) adjusted *p-value* of < 0.05. Principal Component Analysis plots (PCA) were created with the *PlotPCA* function from R using rlog transformed data (Beginner's guide, DESeq2 package, May 13, 2014,

http://www.bioconductor.org/packages/2.14/bioc/vignettes/DESeq2/inst/doc/beginner.pdf). GO enrichment analyses were conducted using the Thalemine tool on Araport (http://www.araport.org). The heatmaps were constructed using the heatmap.2 function of the gplots R package.

Analysis of metal content

Seed (–Fe and +Fe), root and shoot tissues of wild-type plants (Col-0) and *sr45-1* mutant plants were harvested separately. Root tissues were desorbed and washed as previously described (Talke *et al.*, 2006), and seed and shoot tissues were rinsed in distillated water. 1 to 30 mg of dried tissue were digested and prepared as described (Nouet *et al.*, 2015). Metal content was determined by ICP-AES (inductively coupled plasma-atomic emission spectroscopy) (Vista AX, Varian).

Statistical analysis

All data evaluation and statistics were done using GraphPad Prism 7 (GraphPad Software v7.00).

Accession numbers and information

All gene sequences are available through *The Arabidopsis Information Resource* (TAIR, http://www.arabidopsis.org/), with this accession number: *Arabidopsis SR45* (AT1G16610), *AHA2* (AT4G30190), *bHLH100* (AT2G41240), *bHLH101* (AT5G04150), *bHLH11* (AT4G36060), *bHLH18* (AT2G22750), *bHLH19* (AT2G22760), *bHLH20* (AT2G22770), *bHLH25* (AT4G37850), *bHLH38* (AT3G56970), *bHLH39* (AT3G56980), *FIT* (AT2G28160), *FRD3* (AT3G08040), *FRO2* (AT1G01580), *IRT1* (AT4G19690), *MYB15* (AT3G23250), *MYB72* (AT1G56160), *NAS1* (AT5G04950), *NAS2* (AT5G56080), *NAS3* (AT1G09240), *NAS4* (AT1G56430), and *S8H* (AT3G12900). The *Arabidopsis thaliana sr45-1* T-DNA insertion (SALK_004132) and *frd3-7* T-DNA insertion (SALK_122235) lines were available at the SALK collection. The RNA-Seq reads have been deposited in the National Center for Biotechnology Information (NCBI) Sequence Read Archive Database with BioProject identification number [XXX].

Supplemental data

Supplemental Figure S1. Number of potential SR45 targets showing iron deficiency responsiveness.

Supplemental Figure S2. Micronutrient concentrations in *sr45-1* shoots.

Supplemental Figure S3. Macronutrient concentrations in *sr45-1* tissues.

Supplemental Figure S4. Phenotype characterization of wild-type and *sr45-1* seedlings and plants upon iron deficiency and iron excess.

Supplemental Figure S5. Toxicity of manganese and zinc in roots and shoots.

Supplemental Figure S6. Fe uptake machinery activity in *sr45-1* seedlings.

Supplemental Figure S7. Regulation of FIT-interacting coactivators in *sr45-1* adult plants.

Supplemental Figure S8. Transcriptomic analysis in roots upon iron deficiency and sufficiency.

Supplemental Figure S9. Effect of exogenous application of coumarins on *sr45-1* shoots.

Supplemental Figure S10. Effect of irrigation on stem height and flowering.

Supplemental Figure S11. SR45 differentially regulated genes (SDRs) involved in reproductive development.

Supplemental Figure S12. Root length of *sr45-1* seedlings upon iron deficiency and iron excess.

Supplemental Figure S13. Transcriptomic analysis in roots upon iron deficiency and sufficiency.

Supplemental Table S1. Significantly enriched categories among SR45-associated RNAs.

Supplemental Table S2. Lists of differentially expressed genes from all pairwise comparisons described in Figure 4.

Supplemental Table S3. Significantly enriched categories among DEGs identified in roots of WT and *sr45-1* upon iron deficiency and sufficiency.

Supplemental Table S4. Col-0 differentially regulated genes (CDR) and SR45 differentially regulated genes (SDR) from all pairwise comparisons described in Figure 4.

Supplemental Table S5. Significantly enriched categories among CDR genes and SDR genes.

Supplemental Table S6. Comparison of SDR genes identified in roots with SR45-associated RNAs and SDR genes identified in inflorescences.

Supplemental Table S7. List of primers used in this study.

Acknowledgments

We thank Dr. Julien Spielmann for helpful discussions, and Dr. S. Thiriet-Rupert and A. Bertrand for their help with RStudio. We thank Prof. M. Carnol, A. Degueldre and B. Bosman for their help with ICP-AES analyses. Funding was provided by the "Fonds de la Recherche Scientifique–FNRS" (FRFC-1.E049.15, PDR-T.0206.13, CDR-J.0009.17, PDR-T0120.18, CDR-J.0082.21). M.H. is Senior Research Associate of the F.R.S.-FNRS. S.F. was a doctoral fellow (F.R.I.A.). No conflict of interest declared.

Figure legends

Figure 1. Metal concentration, iron staining and H_2O_2 staining in roots upon iron deficiency and iron excess. **(A)** Iron (Fe), **(B)** copper (Cu), **(C)** manganese (Mn) and **(D)** zinc (Zn) concentrations in roots of wild-type (Col-0) and mutant (*sr45-1*) plants grown hydroponically in Hoagland medium supplemented with 0 (deficiency) or 10 (control) µM Fe. Values represent means ± SEM (from one experiment representative of two independent experiments, each including 2 or 3 series of 2 plants per genotype and condition). Data were analyzed by two-way ANOVA followed by Bonferroni multiple comparison post-test. Statistically significant differences between means between genotypes are indicated by stars (* P<0.05, ** P<0,01, *** P<0.001) or between treatments within genotypes by different letters (P<0.05). n.s.: not significant. **(E)** Iron accumulation visualized using Perls staining in roots of Col-0 and *sr45-1*. **(F)** H_2O_2 accumulation stained using DAB in roots of Col-0 and *sr45-1*. The pictures are representative of 2 independent experiments. Arrowheads show Fe or H_2O_2 accumulation in roots. Scale bar: 100 µm.

Figure 2. Phenotypes of wild-type and *sr45-1* plants upon iron deficiency. **(A)** Representative pictures and **(B)** quantification of total chlorophyll content of wild-type (Col-0) and mutant (*sr45-1*) plants grown hydroponically in Hoagland medium supplemented with 0 (deficiency) or 10 (control) µM Fe. Scale bar: 1 cm. **(B)** Ratios of root length and **(C)** shoot fresh weight in *sr45-1 versus* Col-0 plants. Data were analyzed by two-way ANOVA followed by Bonferroni multiple comparison post-test **(B)** or by a t-test **(C-D)**. Statistically significant differences between means between genotypes are indicated by stars (* P<0.05, ** P<0,01, *** P<0.001) or between treatments within genotypes by different letters (P<0.05). n.s.: not significant. Scale bar: 1 cm.

Figure 3. Toxicity of manganese and zinc in *sr45-1* roots. Relative root length of wild-type (Col-0) and mutant (*sr45-1*) plants grown vertically in petri dishes containing Hoagland medium supplemented with iron (10 µM Fe-HBED) but not manganese (0 µM $MnSO_4$) or zinc (0 µM $ZnSO_4$). Root growth is relative to Col-0 at 10 µM Fe-HBED, 5 µM $MnSO_4$ and 1 µM $ZnSO_4$. Values represent means ± SEM (from four independent experiments, each including 2 series of 6 seedlings per genotype and condition). Data were analyzed by two-way ANOVA followed by Bonferroni multiple comparison post-test. Statistically significant differences between means

between genotypes are indicated by stars (*** P<0.001) or between treatments within genotypes by different letters (P<0.05).

Figure 4. Transcriptomic analysis in roots upon iron deficiency and sufficiency. **(A)** Summary statistics of up- (↑) or down-regulated (↓) genes in different pair-wise comparisons. The direction of comparisons is indicated by arrows. Overlaps in Venn diagrams represent deregulated genes in both Col-0 and *sr45-1* roots in respective comparisons (indicated by colors). Right circle: Number of differentially regulated genes solely associated to *sr45-1* roots (SDRs). Left circle: Number of differentially regulated genes solely associated to Col-0 (CDRs). Bar graphs of Gene Ontology (GO) enriched categories in differentially expressed CDR genes **(B)** and SDR genes **(C)**. The enrichment score represents $-\log_{10}(p\text{-value})$. Dissimilar GO terms between genotypes are colored in red (see also **Supplemental Table S5**).

Figure 5. Fe uptake machinery in *sr45-1* seedlings and adult plants. Quantitative RT-PCR analysis of expression of **(A)** *FIT*, **(B)** *AHA2*, **(C)** *FRO2*, **(D)** *IRT1* and **(E)** *FRD3* genes wild-type (Col-0) and mutant (*sr45-1*) seedlings grown vertically in petri dishes containing Hoagland medium supplemented with 0 or 10 µM iron (Fe) **(left panel)** and in roots of wild-type (Col-0) and mutant (*sr45-1*) plants grown hydroponically in Hoagland medium supplemented with 0 or 10 µM Fe (RNA-seq samples) **(right panel)**. Values represent means ± SEM (from four biological replicates, each consisting of 2-6 plants per genotype and condition) and are relative to *At1g58050*. Data were analyzed by two-way ANOVA followed by Bonferroni multiple comparison post-test. Statistically significant differences between means between genotypes are indicated by stars (* P<0.05, ** P<0,01, *** P<0.001) or between treatments within genotypes by different letters (P<0.05). n.s.: not significant.

Figure 6. Effect of exogenous application of coumarins on *sr45-1* roots. **(A)** Relative root growth of wild-type (Col-0) and mutant (*sr45-1*) plants grown vertically in petri dishes containing Hoagland medium supplemented with 10 µM iron (Fe) at various pH (5.7 in presence of Fe-HBED or 7 in presence of $FeCl_3$). Root growth is relative to Col-0 at 10 µM Fe-HBED + DMF (pH 5.7). Values represent means ± SEM (from two independent experiments, each including 3 or 4 series of 6 plants per genotype and condition). Data were analyzed by two-way ANOVA

752 followed by Bonferroni multiple comparison post-test. Statistically significant differences
753 between means between genotypes are indicated by stars (*** P<0.001) or between treatments
754 within genotypes by different letters (P<0.05). **(B)** Iron accumulation and **(C)** H_2O_2 accumulation
755 in roots of wild-type (Col-0) and mutant (*sr45-1*) plants grown vertically in petri dishes
756 containing Hoagland medium supplemented with 0 (deficiency) or 10 (control) µM iron (Fe) at
757 various pH (5.7 in presence of Fe-HBED or 7 in presence of $FeCl_3$). The pictures are
758 representative of two independent experiments. Arrowheads show Fe or H_2O_2 accumulation in
759 roots. Scale bar: 100 µm.
760
761 **Figure 7.** Iron irrigation fully rescues the development of the reproductive tissues. **(A)**
762 Representative pictures of wild-type (Col-0) and mutant (*sr45-1*) siliques, **(B)** silique length, **(C)**
763 representative pictures of wild-type (Col-0) and mutant (*sr45-1*) seeds, **(D)** number of seeds per
764 silique, **(E)** seed mass (for pools of 100 seeds), and **(F)** seed length and width of plants grown in
765 soil and daily irrigated with water without (–Fe) or with an additional treatment consisting of a
766 weekly irrigation with sequestrene (+Fe). Values represent means ± SEM (from three
767 independent experiments with 10-18 siliques pertaining to the main stem [4 plants per genotype
768 and condition] **(B)** or with seeds obtained from 4 plants per genotype and condition **(D-F)**). Scale
769 bars: 1 mm for siliques; 500 µm for seeds. **(G)** Zinc (Zn), **(H)** potassium (K), **(I)** magnesium
770 (Mg) and **(HJ)** manganese (Mn) concentration in seeds (–Fe or +Fe) of wild-type (Col-0) and
771 mutant (*sr45-1*) plants. Values represent means ± SEM (from three independent experiments with
772 seeds obtained from 4 plants per genotype and condition). For each experiment, data were
773 analyzed by two-way ANOVA followed by Bonferroni multiple comparison post-test.
774 Statistically significant differences between means are indicated by stars (* P<0.05, ** P<0,01,
775 *** P<0.001) or different letters (P<0.05). n.s.: not significant. **(F)** was obtained by performing
776 statistical analysis for both seed length and seed width independently and then by displaying the
777 results in a single graph.
778
779 **Literature cited**

780 Albaqami, M., Laluk, K., and Reddy, A.S.N. (2019). The Arabidopsis splicing regulator SR45
781 confers salt tolerance in a splice isoform-dependent manner. Plant Mol Biol 100, 379-390.

782 Ali, G.S., Palusa, S.G., Golovkin, M., Prasad, J., Manley, J.L., and Reddy, A.S. (2007).
783 Regulation of plant developmental processes by a novel splicing factor. PLoS One 2, e471.
784 Babst, B.A., Gao, F., Acosta-Gamboa, L.M., Karve, A., Schueller, M.J., and Lorence, A. (2019).
785 Three NPF genes in Arabidopsis are necessary for normal nitrogen cycling under low nitrogen
786 stress. Plant Physiol Biochem 143, 1-10.
787 Baliardini, C., Meyer, C.L., Salis, P., Saumitou-Laprade, P., and Verbruggen, N. (2015).
788 CATION EXCHANGER1 Cosegregates with Cadmium Tolerance in the Metal
789 Hyperaccumulator Arabidopsis halleri and Plays a Role in Limiting Oxidative Stress in
790 Arabidopsis Spp. Plant Physiol 169, 549-559.
791 Barberon, M., Vermeer, J.E., De Bellis, D., Wang, P., Naseer, S., Andersen, T.G., Humbel, B.M.,
792 Nawrath, C., Takano, J., Salt, D.E., and Geldner, N. (2016). Adaptation of Root Function by
793 Nutrient-Induced Plasticity of Endodermal Differentiation. Cell 164, 447-459.
794 Barta, A., Kalyna, M., and Reddy, A.S. (2010). Implementing a rational and consistent
795 nomenclature for serine/arginine-rich protein splicing factors (SR proteins) in plants. Plant Cell
796 22, 2926-2929.
797 Baxter, I., Hosmani, P.S., Rus, A., Lahner, B., Borevitz, J.O., Muthukumar, B., Mickelbart, M.V.,
798 Schreiber, L., Franke, R.B., and Salt, D.E. (2009). Root suberin forms an extracellular barrier that
799 affects water relations and mineral nutrition in Arabidopsis. PLoS Genet 5, e1000492.
800 Bolger, A.M., Lohse, M., and Usadel, B. (2014). Trimmomatic: a flexible trimmer for Illumina
801 sequence data. Bioinformatics 30, 2114-2120.
802 Califice, S., Baurain, D., Hanikenne, M., and Motte, P. (2012). A single ancient origin for
803 prototypical serine/arginine-rich splicing factors. Plant Physiol 158, 546-560.
804 Carvalho, R.F., Carvalho, S.D., and Duque, P. (2010). The plant-specific SR45 protein negatively
805 regulates glucose and ABA signaling during early seedling development in Arabidopsis. Plant
806 Physiol 154, 772-783.
807 Carvalho, R.F., Szakonyi, D., Simpson, C.G., Barbosa, I.C., Brown, J.W., Baena-González, E.,
808 and Duque, P. (2016). The Arabidopsis SR45 Splicing Factor, a Negative Regulator of Sugar
809 Signaling, Modulates SNF1-Related Protein Kinase 1 Stability. Plant Cell 28, 1910-1925.
810 Castaings, L., Caquot, A., Loubet, S., and Curie, C. (2016). The high-affinity metal Transporters
811 NRAMP1 and IRT1 Team up to Take up Iron under Sufficient Metal Provision. Sci Rep 6,
812 37222.

Chamala, S., Feng, G., Chavarro, C., and Barbazuk, W.B. (2015). Genome-wide identification of evolutionarily conserved alternative splicing events in flowering plants. Front Bioeng Biotechnol 3, 33.

Charlier, J.B., Polese, C., Nouet, C., Carnol, M., Bosman, B., Krämer, U., Motte, P., and Hanikenne, M. (2015). Zinc triggers a complex transcriptional and post-transcriptional regulation of the metal homeostasis gene FRD3 in Arabidopsis relatives. J Exp Bot 66, 3865-3878.

Chen, S.L., Rooney, T.J., Hu, A.R., Beard, H.S., Garrett, W.M., Mangalath, L.M., Powers, J.J., Cooper, B., and Zhang, X.N. (2019). Quantitative Proteomics Reveals a Role for SERINE/ARGININE-Rich 45 in Regulating RNA Metabolism and Modulating Transcriptional Suppression via the ASAP Complex in Arabidopsis thaliana. Front Plant Sci 10, 1116.

Chen, T., Cui, P., Chen, H., Ali, S., Zhang, S., and Xiong, L. (2013). A KH-domain RNA-binding protein interacts with FIERY2/CTD phosphatase-like 1 and splicing factors and is important for pre-mRNA splicing in Arabidopsis. PLoS Genet 9, e1003875.

Chezem, W.R., Memon, A., Li, F.S., Weng, J.K., and Clay, N.K. (2017). SG2-Type R2R3-MYB Transcription Factor MYB15 Controls Defense-Induced Lignification and Basal Immunity in Arabidopsis. Plant Cell 29, 1907-1926.

Colangelo, E.P., and Guerinot, M.L. (2004). The essential basic helix-loop-helix protein FIT1 is required for the iron deficiency response. Plant Cell 16, 3400-3412.

Cui, Y., Chen, C.L., Cui, M., Zhou, W.J., Wu, H.L., and Ling, H.Q. (2018). Four IVa bHLH Transcription Factors Are Novel Interactors of FIT and Mediate JA Inhibition of Iron Uptake in Arabidopsis. Mol Plant 11, 1166-1183.

Curie, C., and Mari, S. (2017). New routes for plant iron mining. New Phytol 214, 521-525.

Czechowski, T., Stitt, M., Altmann, T., Udvardi, M.K., and Scheible, W.R. (2005). Genome-wide identification and testing of superior reference genes for transcript normalization in Arabidopsis. Plant Physiol 139, 5-17.

Dong, C., He, F., Berkowitz, O., Liu, J., Cao, P., Tang, M., Shi, H., Wang, W., Li, Q., Shen, Z., Whelan, J., and Zheng, L. (2018). Alternative Splicing Plays a Critical Role in Maintaining Mineral Nutrient Homeostasis in Rice (Oryza sativa). Plant Cell 30, 2267-2285.

Dučić, T., and Polle, A. (2007). Manganese toxicity in two varieties of Douglas fir (Pseudotsuga menziesii var. viridis and glauca) seedlings as affected by phosphorus supply. Functional Plant Biology 34, 31-40.

844 Durrett, T.P., Gassmann, W., and Rogers, E.E. (2007). The FRD3-mediated efflux of citrate into
845 the root vasculature is necessary for efficient iron translocation. Plant Physiol 144, 197-205.
846 El-Ashgar, N.M., El-Basioni, A., El-Nahhal, I.M., Zourob, S.M., El-Agez, T.M., and Taya, S.A.
847 (2012). Sol-Gel Thin Films Immobilized with Bromocresol Purple pH-Sensitive Indicator in
848 Presence of Surfactants. ISRN Analytical Chemistry 2012.
849 Fan, S.C., Lin, C.S., Hsu, P.K., Lin, S.H., and Tsay, Y.F. (2009). The Arabidopsis nitrate
850 transporter NRT1.7, expressed in phloem, is responsible for source-to-sink remobilization of
851 nitrate. Plant Cell 21, 2750-2761.
852 Fourcroy, P., Sisó-Terraza, P., Sudre, D., Saviron, M., Reyt, G., Gaymard, F., Abadía, A.,
853 Abadia, J., Álvarez-Fernández, A., and Briat, J.F. (2014). Involvement of the ABCG37
854 transporter in secretion of scopoletin and derivatives by Arabidopsis roots in response to iron
855 deficiency. New Phytol 201, 155-167.
856 Fukao, Y., Ferjani, A., Tomioka, R., Nagasaki, N., Kurata, R., Nishimori, Y., Fujiwara, M., and
857 Maeshima, M. (2011). iTRAQ analysis reveals mechanisms of growth defects due to excess zinc
858 in Arabidopsis. Plant Physiol 155, 1893-1907.
859 García, M.J., Lucena, C., Romera, F.J., Alcántara, E., and Pérez-Vicente, R. (2010). Ethylene and
860 nitric oxide involvement in the up-regulation of key genes related to iron acquisition and
861 homeostasis in Arabidopsis. J Exp Bot 61, 3885-3899.
862 Geldner, N. (2013). The endodermis. Annu Rev Plant Biol 64, 531-558.
863 Glaring, M.A., Zygadlo, A., Thorneycroft, D., Schulz, A., Smith, S.M., Blennow, A., and
864 Baunsgaard, L. (2007). An extra-plastidial alpha-glucan, water dikinase from Arabidopsis
865 phosphorylates amylopectin in vitro and is not necessary for transient starch degradation. J Exp
866 Bot 58, 3949-3960.
867 Golovkin, M., and Reddy, A.S. (1999). An SC35-like protein and a novel serine/arginine-rich
868 protein interact with Arabidopsis U1-70K protein. J Biol Chem 274, 36428-36438.
869 Green, L.S., and Rogers, E.E. (2004). FRD3 controls iron localization in Arabidopsis. Plant
870 Physiol 136, 2523-2531.
871 Guo, W., Nazim, H., Liang, Z., and Yang, D. (2016). Magnesium deficiency in plants: An urgent
872 problem. The Crop Journal 4, 83-91.
873 Hanikenne, M., Esteves, S.M., Fanara, S., and Rouached, H. (2021). Coordinated homeostasis of
874 essential mineral nutrients: a focus on iron. J Exp Bot 72, 2136-2153.

875 Hanikenne, M., Talke, I.N., Haydon, M.J., Lanz, C., Nolte, A., Motte, P., Kroymann, J., Weigel,
876 D., and Krämer, U. (2008). Evolution of metal hyperaccumulation required cis-regulatory
877 changes and triplication of HMA4. Nature 453, 391-395.
878 Haydon, M.J., Kawachi, M., Wirtz, M., Hillmer, S., Hell, R., and Krämer, U. (2012). Vacuolar
879 nicotianamine has critical and distinct roles under iron deficiency and for zinc sequestration in
880 Arabidopsis. Plant Cell 24, 724-737.
881 Hindt, M.N., Akmakjian, G.Z., Pivarski, K.L., Punshon, T., Baxter, I., Salt, D.E., and Guerinot,
882 M.L. (2017). BRUTUS and its paralogs, BTS LIKE1 and BTS LIKE2, encode important negative
883 regulators of the iron deficiency response in Arabidopsis thaliana. Metallomics 9, 876-890.
884 Ivanov, R., Brumbarova, T., and Bauer, P. (2012). Fitting into the harsh reality: regulation of
885 iron-deficiency responses in dicotyledonous plants. Mol Plant 5, 27-42.
886 Jakoby, M., Wang, H.Y., Reidt, W., Weisshaar, B., and Bauer, P. (2004). FRU (BHLH029) is
887 required for induction of iron mobilization genes in Arabidopsis thaliana. FEBS Lett 577, 528-
888 534.
889 Jeong, S. (2017). SR Proteins: Binders, Regulators, and Connectors of RNA. Mol Cells 40, 1-9.
890 Kailasam, S., Wang, Y., Lo, J.C., Chang, H.F., and Yeh, K.C. (2018). S-Nitrosoglutathione
891 works downstream of nitric oxide to mediate iron-deficiency signaling in Arabidopsis. Plant J 94,
892 157-168.
893 Kamiya, T., Borghi, M., Wang, P., Danku, J.M., Kalmbach, L., Hosmani, P.S., Naseer, S.,
894 Fujiwara, T., Geldner, N., and Salt, D.E. (2015). The MYB36 transcription factor orchestrates
895 Casparian strip formation. Proc Natl Acad Sci U S A 112, 10533-10538.
896 Kawachi, M., Kobae, Y., Mori, H., Tomioka, R., Lee, Y., and Maeshima, M. (2009). A mutant
897 strain Arabidopsis thaliana that lacks vacuolar membrane zinc transporter MTP1 revealed the
898 latent tolerance to excessive zinc. Plant Cell Physiol 50, 1156-1170.
899 Kobayashi, T., Nagasaka, S., Senoura, T., Itai, R.N., Nakanishi, H., and Nishizawa, N.K. (2013).
900 Iron-binding haemerythrin RING ubiquitin ligases regulate plant iron responses and
901 accumulation. Nat Commun 4, 2792.
902 Laloum, T., Martín, G., and Duque, P. (2018). Alternative Splicing Control of Abiotic Stress
903 Responses. Trends Plant Sci 23, 140-150.
904 Le, C.T., Brumbarova, T., Ivanov, R., Stoof, C., Weber, E., Mohrbacher, J., Fink-Straube, C., and
905 Bauer, P. (2016). ZINC FINGER OF ARABIDOPSIS THALIANA12 (ZAT12) Interacts with

906 FER-LIKE IRON DEFICIENCY-INDUCED TRANSCRIPTION FACTOR (FIT) Linking Iron
907 Deficiency and Oxidative Stress Responses. Plant Physiol 170, 540-557.
908 Lei, Y., Korpelainen, H., and Li, C. (2007). Physiological and biochemical responses to high Mn
909 concentrations in two contrasting Populus cathayana populations. Chemosphere 68, 686-694.
910 Li, J., Zhang, M., Sun, J., Mao, X., Wang, J., Liu, H., Zheng, H., Li, X., Zhao, H., and Zou, D.
911 (2020). Heavy Metal Stress-Associated Proteins in Rice and Arabidopsis: Genome-Wide
912 Identification, Phylogenetics, Duplication, and Expression Profiles Analysis. Front Genet 11,
913 477.
914 Lichtenthaler, H.K., and Buschmann, C. (2001). Chlorophylls and Carotenoids: Measurement and
915 Characterization by UV-VIS Spectroscopy. Current Protocols in Food Analytical Chemistry F4,
916 1– F4.3.8.
917 Lingam, S., Mohrbacher, J., Brumbarova, T., Potuschak, T., Fink-Straube, C., Blondet, E.,
918 Genschik, P., and Bauer, P. (2011). Interaction between the bHLH transcription factor FIT and
919 ETHYLENE INSENSITIVE3/ETHYLENE INSENSITIVE3-LIKE1 reveals molecular linkage
920 between the regulation of iron acquisition and ethylene signaling in Arabidopsis. Plant Cell 23,
921 1815-1829.
922 Liu, M., Liu, X.X., He, X.L., Liu, L.J., Wu, H., Tang, C.X., Zhang, Y.S., and Jin, C.W. (2017a).
923 Ethylene and nitric oxide interact to regulate the magnesium deficiency-induced root hair
924 development in Arabidopsis. New Phytol 213, 1242-1256.
925 Liu, M., Zhang, H., Fang, X., Zhang, Y., and Jin, C. (2018). Auxin Acts Downstream of Ethylene
926 and Nitric Oxide to Regulate Magnesium Deficiency-Induced Root Hair Development in
927 Arabidopsis thaliana. Plant Cell Physiol 59, 1452-1465.
928 Liu, W., Sun, Q., Wang, K., Du, Q., and Li, W.X. (2017b). Nitrogen Limitation Adaptation
929 (NLA) is involved in source-to-sink remobilization of nitrate by mediating the degradation of
930 NRT1.7 in Arabidopsis. New Phytol 214, 734-744.
931 Long, T.A., Tsukagoshi, H., Busch, W., Lahner, B., Salt, D.E., and Benfey, P.N. (2010). The
932 bHLH transcription factor POPEYE regulates response to iron deficiency in Arabidopsis roots.
933 Plant Cell 22, 2219-2236.
934 Love, M.I., Huber, W., and Anders, S. (2014). Moderated estimation of fold change and
935 dispersion for RNA-seq data with DESeq2. Genome Biology 15, 550.

936 Manley, J.L., and Krainer, A.R. (2010). A rational nomenclature for serine/arginine-rich protein
937 splicing factors (SR proteins). Genes Dev 24, 1073-1074.
938 Marschner, H., and Marschner, P. (2012). Marschner's Mineral Nutrition of Higher Plants (3rd
939 edition). Academic Press.
940 Meyer, K., Koester, T., and Staiger, D. (2015). Pre-mRNA Splicing in Plants: In Vivo Functions
941 of RNA-Binding Proteins Implicated in the Splicing Process. Biomolecules 5, 1717-1740.
942 Millaleo, R., Reyes-Díaz, M., Alberdi, M., Ivanov, A.G., Krol, M., and Hüner, N.P. (2013).
943 Excess manganese differentially inhibits photosystem I versus II in Arabidopsis thaliana. J Exp
944 Bot 64, 343-354.
945 Mladenka, P., Macáková, K., Zatloukalová, L., Reháková, Z., Singh, B.K., Prasad, A.K., Parmar,
946 V.S., Jahodár, L., Hrdina, R., and Saso, L. (2010). In vitro interactions of coumarins with iron.
947 Biochimie 92, 1108-1114.
948 Morrissey, J., Baxter, I.R., Lee, J., Li, L., Lahner, B., Grotz, N., Kaplan, J., Salt, D.E., and
949 Guerinot, M.L. (2009). The ferroportin metal efflux proteins function in iron and cobalt
950 homeostasis in Arabidopsis. Plant Cell 21, 3326-3338.
951 Nouet, C., Charlier, J.B., Carnol, M., Bosman, B., Farnir, F., Motte, P., and Hanikenne, M.
952 (2015). Functional analysis of the three HMA4 copies of the metal hyperaccumulator Arabidopsis
953 halleri. J Exp Bot 66, 5783-5795.
954 Nouet, C., Motte, P., and Hanikenne, M. (2011). Chloroplastic and mitochondrial metal
955 homeostasis. Trends Plant Sci 16, 395-404.
956 Palmer, C.M., Hindt, M.N., Schmidt, H., Clemens, S., and Guerinot, M.L. (2013). MYB10 and
957 MYB72 are required for growth under iron-limiting conditions. PLoS Genet 9, e1003953.
958 Palusa, S.G., Ali, G.S., and Reddy, A.S. (2007). Alternative splicing of pre-mRNAs of
959 Arabidopsis serine/arginine-rich proteins: regulation by hormones and stresses. Plant J 49, 1091-
960 1107.
961 Palusa, S.G., and Reddy, A.S. (2010). Extensive coupling of alternative splicing of pre-mRNAs
962 of serine/arginine (SR) genes with nonsense-mediated decay. New Phytol 185, 83-89.
963 Petridis, A., Döll, S., Nichelmann, L., Bilger, W., and Mock, H.P. (2016). Arabidopsis thaliana
964 G2-LIKE FLAVONOID REGULATOR and BRASSINOSTEROID ENHANCED
965 EXPRESSION1 are low-temperature regulators of flavonoid accumulation. New Phytol 211,
966 912-925.

967 Pfaffl, M.W. (2001). A new mathematical model for relative quantification in real-time RT-PCR.
968 Nucleic Acids Res 29, e45.
969 Pirone, C., Gurrieri, L., Gaiba, I., Adamiano, A., Valle, F., Trost, P., and Sparla, F. (2017). The
970 analysis of the different functions of starch-phosphorylating enzymes during the development of
971 Arabidopsis thaliana plants discloses an unexpected role for the cytosolic isoform GWD2.
972 Physiol Plant 160, 447-457.
973 Rajniak, J., Giehl, R.F.H., Chang, E., Murgia, I., von Wirén, N., and Sattely, E.S. (2018).
974 Biosynthesis of redox-active metabolites in response to iron deficiency in plants. Nat Chem Biol
975 14, 442-450.
976 Ravet, K., Touraine, B., Boucherez, J., Briat, J.F., Gaymard, F., and Cellier, F. (2009). Ferritins
977 control interaction between iron homeostasis and oxidative stress in Arabidopsis. Plant J 57, 400-
978 412.
979 Remy, E., Cabrito, T.R., Batista, R.A., Hussein, M.A., Teixeira, M.C., Athanasiadis, A., Sá-
980 Correia, I., and Duque, P. (2014). Intron retention in the 5'UTR of the novel ZIF2 transporter
981 enhances translation to promote zinc tolerance in Arabidopsis. PLoS Genet 10, e1004375.
982 Reyt, G., Boudouf, S., Boucherez, J., Gaymard, F., and Briat, J.F. (2015). Iron- and ferritin-
983 dependent reactive oxygen species distribution: impact on Arabidopsis root system architecture.
984 Mol Plant 8, 439-453.
985 Robinson, N.J., Procter, C.M., Connolly, E.L., and Guerinot, M.L. (1999). A ferric-chelate
986 reductase for iron uptake from soils. Nature 397, 694-697.
987 Rodríguez-Celma, J., Connorton, J.M., Kruse, I., Green, R.T., Franceschetti, M., Chen, Y.T., Cui,
988 Y., Ling, H.Q., Yeh, K.C., and Balk, J. (2019). Arabidopsis BRUTUS-LIKE E3 ligases
989 negatively regulate iron uptake by targeting transcription factor FIT for recycling. Proc Natl Acad
990 Sci U S A 116, 17584-17591.
991 Römheld, V., and Marschner, H. (1986). Evidence for a specific uptake system for iron
992 phytosiderophores in roots of grasses. Plant Physiol 80, 175-180.
993 Roschzttardtz, H., Conéjéro, G., Curie, C., and Mari, S. (2009). Identification of the endodermal
994 vacuole as the iron storage compartment in the Arabidopsis embryo. Plant Physiol 151, 1329-
995 1338.

996 Roschzttardtz, H., Seguela-Arnaud, M., Briat, J.F., Vert, G., and Curie, C. (2011). The FRD3
997 citrate effluxer promotes iron nutrition between symplastically disconnected tissues throughout
998 Arabidopsis development. Plant Cell 23, 2725-2737.
999 Santi, S., and Schmidt, W. (2009). Dissecting iron deficiency-induced proton extrusion in
1000 Arabidopsis roots. New Phytol 183, 1072-1084.
1001 Scheepers, M., Spielmann, J., Boulanger, M., Carnol, M., Bosman, B., De Pauw, E.,
1002 Goormaghtigh, E., Motte, P., and Hanikenne, M. (2020). Intertwined metal homeostasis,
1003 oxidative and biotic stress responses in the Arabidopsis frd3 mutant. Plant J.
1004 Schmidt, H., Günther, C., Weber, M., Spörlein, C., Loscher, S., Böttcher, C., Schobert, R., and
1005 Clemens, S. (2014). Metabolome analysis of Arabidopsis thaliana roots identifies a key metabolic
1006 pathway for iron acquisition. PLoS One 9, e102444.
1007 Schvartzman, M.S., Corso, M., Fataftah, N., Scheepers, M., Nouet, C., Bosman, B., Carnol, M.,
1008 Motte, P., Verbruggen, N., and Hanikenne, M. (2018). Adaptation to high zinc depends on
1009 distinct mechanisms in metallicolous populations of Arabidopsis halleri. New Phytol 218, 269-
1010 282.
1011 Selote, D., Samira, R., Matthiadis, A., Gillikin, J.W., and Long, T.A. (2015). Iron-binding E3
1012 ligase mediates iron response in plants by targeting basic helix-loop-helix transcription factors.
1013 Plant Physiol 167, 273-286.
1014 Shang, X., Cao, Y., and Ma, L. (2017). Alternative Splicing in Plant Genes: A Means of
1015 Regulating the Environmental Fitness of Plants. Int J Mol Sci 18.
1016 Shanmugam, V., Lo, J.C., Wu, C.L., Wang, S.L., Lai, C.C., Connolly, E.L., Huang, J.L., and
1017 Yeh, K.C. (2011). Differential expression and regulation of iron-regulated metal transporters in
1018 Arabidopsis halleri and Arabidopsis thaliana - the role in zinc tolerance. New Phytol 190, 125-
1019 137.
1020 Singh, S.K., and Reddy, V.R. (2017). Potassium Starvation Limits Soybean Growth More than
1021 the Photosynthetic Processes across CO2 Levels. Front Plant Sci 8, 991.
1022 Sivitz, A.B., Hermand, V., Curie, C., and Vert, G. (2012). Arabidopsis bHLH100 and bHLH101
1023 control iron homeostasis via a FIT-independent pathway. PLoS One 7, e44843.
1024 Siwinska, J., Siatkowska, K., Olry, A., Grosjean, J., Hehn, A., Bourgaud, F., Meharg, A.A.,
1025 Carey, M., Lojkowska, E., and Ihnatowicz, A. (2018). Scopoletin 8-hydroxylase: a novel enzyme

involved in coumarin biosynthesis and iron-deficiency responses in Arabidopsis. J Exp Bot 69, 1735-1748.

Song, W.Y., Choi, K.S., Kim, D.Y., Geisler, M., Park, J., Vincenzetti, V., Schellenberg, M., Kim, S.H., Lim, Y.P., Noh, E.W., Lee, Y., and Martinoia, E. (2010). Arabidopsis PCR2 is a zinc exporter involved in both zinc extrusion and long-distance zinc transport. Plant Cell 22, 2237-2252.

Spielmann, J., Ahmadi, H., Scheepers, M., Weber, M., Nitsche, S., Carnol, M., Bosman, B., Kroymann, J., Motte, P., Clemens, S., and Hanikenne, M. (2020). The two copies of the zinc and cadmium ZIP6 transporter of Arabidopsis halleri have distinct effects on cadmium tolerance. Plant Cell Environ 43, 2143-2157.

Stacey, M.G., Patel, A., McClain, W.E., Mathieu, M., Remley, M., Rogers, E.E., Gassmann, W., Blevins, D.G., and Stacey, G. (2008). The Arabidopsis AtOPT3 protein functions in metal homeostasis and movement of iron to developing seeds. Plant Physiol 146, 589-601.

Talke, I.N., Hanikenne, M., and Krämer, U. (2006). Zinc-dependent global transcriptional control, transcriptional deregulation, and higher gene copy number for genes in metal homeostasis of the hyperaccumulator Arabidopsis halleri. Plant Physiol 142, 148-167.

Tehseen, M., Cairns, N., Sherson, S., and Cobbett, C.S. (2010). Metallochaperone-like genes in Arabidopsis thaliana. Metallomics 2, 556-564.

Thomine, S., and Vert, G. (2013). Iron transport in plants: better be safe than sorry. Curr Opin Plant Biol 16, 322-327.

Tsai, H.H., Rodríguez-Celma, J., Lan, P., Wu, Y.C., Vélez-Bermúdez, I.C., and Schmidt, W. (2018). Scopoletin 8-Hydroxylase-Mediated Fraxetin Production Is Crucial for Iron Mobilization. Plant Physiol 177, 194-207.

Verbruggen, N., and Hermans, C. (2013). Physiological and molecular responses to magnesium nutritional imbalance in plants. Plant and Soil 368, 87-99.

Vert, G., Grotz, N., Dédaldéchamp, F., Gaymard, F., Guerinot, M.L., Briat, J.F., and Curie, C. (2002). IRT1, an Arabidopsis transporter essential for iron uptake from the soil and for plant growth. Plant Cell 14, 1223-1233.

Wang, N., Cui, Y., Liu, Y., Fan, H., Du, J., Huang, Z., Yuan, Y., Wu, H., and Ling, H.Q. (2013). Requirement and functional redundancy of Ib subgroup bHLH proteins for iron deficiency responses and uptake in Arabidopsis thaliana. Mol Plant 6, 503-513.

1057 Wintermans, J.F., and de Mots, A. (1965). Spectrophotometric characteristics of chlorophylls a
1058 and b and their pheophytins in ethanol. Biochim Biophys Acta 109, 448-453.
1059 Xing, D., Wang, Y., Hamilton, M., Ben-Hur, A., and Reddy, A.S. (2015). Transcriptome-Wide
1060 Identification of RNA Targets of Arabidopsis SERINE/ARGININE-RICH45 Uncovers the
1061 Unexpected Roles of This RNA Binding Protein in RNA Processing. Plant Cell 27, 3294-3308.
1062 Yi, Y., and Guerinot, M.L. (1996). Genetic evidence that induction of root Fe(III) chelate
1063 reductase activity is necessary for iron uptake under iron deficiency. Plant J 10, 835-844.
1064 Yuan, Y., Wu, H., Wang, N., Li, J., Zhao, W., Du, J., Wang, D., and Ling, H.Q. (2008). FIT
1065 interacts with AtbHLH38 and AtbHLH39 in regulating iron uptake gene expression for iron
1066 homeostasis in Arabidopsis. Cell Res 18, 385-397.
1067 Zhang, W., Du, B., Liu, D., and Qi, X. (2014). Splicing factor SR34b mutation reduces cadmium
1068 tolerance in Arabidopsis by regulating iron-regulated transporter 1 gene. Biochem Biophys Res
1069 Commun 455, 312-317.
1070 Zhang, X.N., and Mount, S.M. (2009). Two alternatively spliced isoforms of the Arabidopsis
1071 SR45 protein have distinct roles during normal plant development. Plant Physiol 150, 1450-1458.
1072 Zhang, X.N., Shi, Y., Powers, J.J., Gowda, N.B., Zhang, C., Ibrahim, H.M.M., Ball, H.B., Chen,
1073 S.L., Lu, H., and Mount, S.M. (2017). Transcriptome analyses reveal SR45 to be a neutral
1074 splicing regulator and a suppressor of innate immunity in Arabidopsis thaliana. BMC Genomics
1075 18, 772.

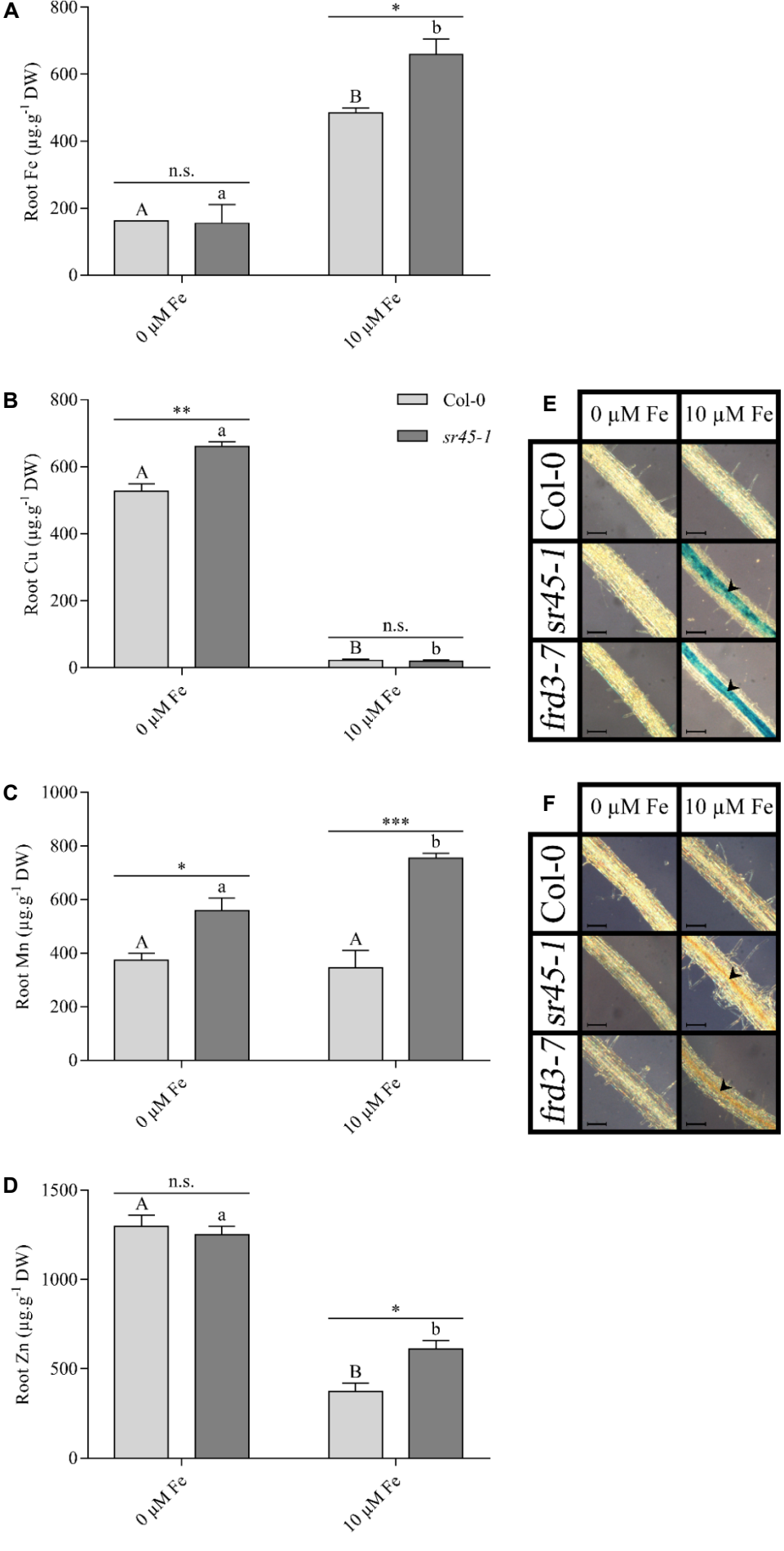
A
Root Fe (µg.g-1 DW)
800
600
400
200
0
n.s.
*
A
a
B
b
0 µM Fe
10 µM Fe
B
Root Cu (µg.g-1 DW)
**
n.s.
Col-0
sr45-1
C
Root Mn (µg.g-1 DW)
1000
***
D
Root Zn (µg.g-1 DW)
1500
1000
500
E
F
0 µM Fe
10 µM Fe
Col-0
sr45-1
frd3-7

Figure 1

Figure 1. Metal concentration, iron staining and H_2O_2 staining in roots upon iron deficiency and iron excess. **(A)** Iron (Fe), **(B)** copper (Cu), **(C)** manganese (Mn) and **(D)** zinc (Zn) concentration in roots of wild-type (Col-0) and mutant (*sr45-1*) plants grown hydroponically in Hoagland medium supplemented with 0 (deficiency) or 10 (control) µM Fe. Values represent means ± SEM (from one experiment representative of two independent experiments, each including 2 or 3 series of 2 plants per genotype and condition). Data were analyzed by two-way ANOVA followed by Bonferroni multiple comparison post-test. Statistically significant differences between means between genotypes are indicated by stars (* P<0.05, ** P<0,01, *** P<0.001) or between treatments within genotypes by different letters (P<0.05). **(E)** Iron accumulation visualized using Perls staining in roots of Col-0 and *sr45-1*. **(F)** H_2O_2 accumulation stained using DAB in roots of Col-0 and *sr45-1*. The pictures are representative of 2 independent experiments. Arrowheads show Fe or H_2O_2 accumulation in roots. Scale bar: 100 µm.

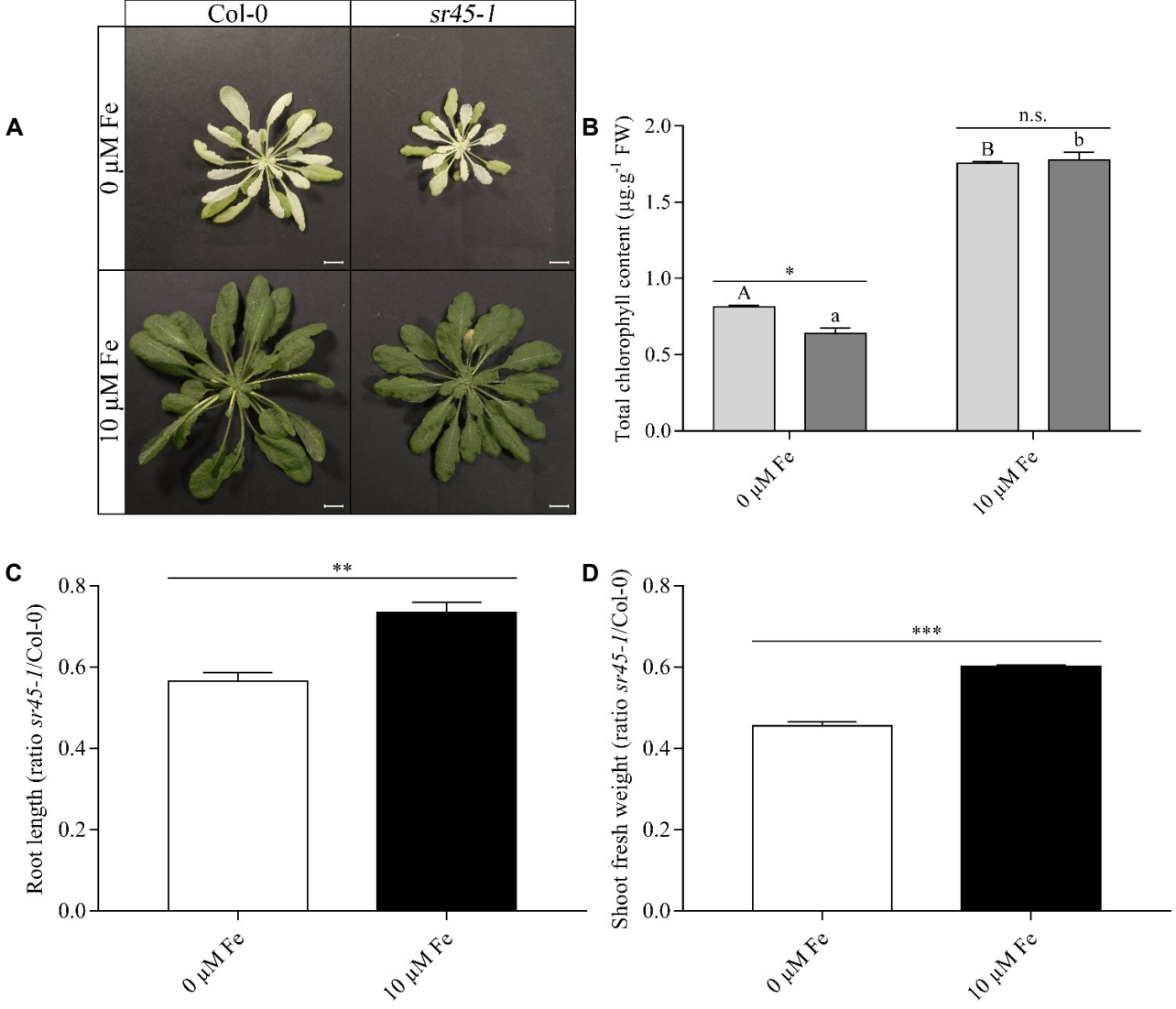
A
Col-0
sr45-1
0 µM Fe
10 µM Fe
B
Total chlorophyll content (µg.g-1 FW)
2.0
1.5
1.0
0.5
0.0
*
A
a
n.s.
B
b
0 µM Fe
10 µM Fe
C
Root length (ratio sr45-1/Col-0)
0.8
0.6
0.4
0.2
0.0
**
0 µM Fe
10 µM Fe
D
Shoot fresh weight (ratio sr45-1/Col-0)
0.8
0.6
0.4
0.2
0.0
***
0 µM Fe
10 µM Fe

Figure 2

Figure 2. Phenotypes of aerial parts of wild-type and *sr45-1* plants upon iron deficiency. **(A)** Representative pictures and **(B)** quantification of total chlorophyll content of wild-type (Col-0) and mutant (*sr45-1*) plants grown hydroponically in Hoagland medium supplemented with 0 (deficiency) or 10 (control) µM Fe. Scale bar: 1 cm. **(B)** Ratios of root length and **(C)** shoot fresh weight in *sr45-1 versus* Col-0 plants. Data were analyzed by two-way ANOVA followed by Bonferroni multiple comparison post-test **(B)** or by a t-test **(C-D)**. Statistically significant differences between means between genotypes are indicated by stars (* $P<0.05$, ** $P<0,01$, *** $P<0.001$) or between treatments within genotypes by different letters ($P<0.05$). Scale bar: 1 cm.

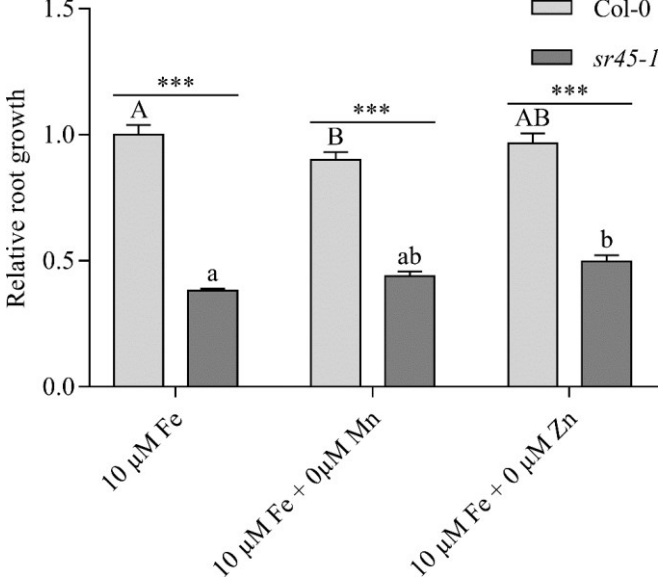
Col-0
sr45-1
Relative root growth
1.5
1.0
0.5
0.0
***
***
***
A
B
AB
a
ab
b
10 μM Fe
10 μM Fe + 0μM Mn
10 μM Fe + 0 μM Zn

Figure 3

Figure 3. Toxicity of iron, manganese and zinc in roots. Relative root length of wild-type (Col-0) and mutant (*sr45-1*) plants grown vertically in petri dishes containing Hoagland medium supplemented with iron (10 µM Fe-HBED) but not manganese (0 µM $MnSO_4$) or zinc (0 µM $ZnSO_4$). Root growth is relative to Col-0 at 10 µM Fe-HBED, 5 µM $MnSO_4$ and 1 µM $ZnSO_4$. Values represent means ± SEM (from four independent experiments, each including 2 series of 6 seedlings per genotype and condition). Data were analyzed by two-way ANOVA followed by Bonferroni multiple comparison post-test. Statistically significant differences between means between genotypes are indicated by stars (*** $P<0.001$) or between treatments within genotypes by different letters ($P<0.05$).


A
Col-0
829
1613
sr45-1
387
Col-0
1396
1046
sr45-1
304
Col-0 – 10 µM Fe
sr45-1 – 10 µM Fe
Col-0 – 0 µM Fe
sr45-1 – 0 µM Fe
↑10 ↓19
↑719 ↓1723
↑557 ↓793
↑17 ↓32
7696
↓1220
↑712
↓1304
Col-0
759
1173
sr45-1
827
Col-0
841
1091
sr45-1
259
B
response to chemical
response to stimulus
response to oxygen-containing compound
response to stress
secondary metabolic process
response to acid chemical
response to wounding
response to organic substance
response to endogenous stimulus
response to hormone
response to abiotic stimulus
cell wall organization or biogenesis
response to jasmonic acid
aromatic amino acid family metabolic process
cellular response to chemical stimulus
cellular response to hypoxia
cellular response to oxygen levels
cellular response to decreased oxygen levels
response to drug
hormone metabolic process
regulation of hormone levels
response to hypoxia
hormone biosynthetic process
cell wall organization
toxin metabolic process
response to decreased oxygen levels
response to chitin
response to oxygen levels
response to ethylene
jasmonic acid mediated signaling pathway
secondary metabolite biosynthetic process
external encapsulating structure organization
carbohydrate metabolic process
cellular response to ethylene stimulus
phenylpropanoid metabolic process
regulation of biological quality
indolalkylamine metabolic process
tryptophan metabolic process
phenylpropanoid biosynthetic process
oxoacid metabolic process
response to water deprivation
carboxylic acid biosynthetic process
organic acid biosynthetic process
indole-containing compound metabolic process
lignin metabolic process
organic acid metabolic process
ethylene-activated signaling pathway
alpha-amino acid metabolic process
cellular response to endogenous stimulus
response to water
response to red light
aromatic compound biosynthetic process
plant-type cell wall organization or biogenesis
GO enriched categories
0
5
10
Enrichment score
C
response to chemical
response to stimulus
response to oxygen-containing compound
response to abiotic stimulus
response to hypoxia
cellular response to hypoxia
cellular response to oxygen levels
cellular response to decreased oxygen levels
response to decreased oxygen levels
response to oxygen levels
response to drug
response to organic substance
response to stress
regulation of biological quality
response to chitin
response to acid chemical
cellular response to chemical stimulus
response to endogenous stimulus
response to hormone
secondary metabolic process
chemical homeostasis
response to organonitrogen compound
GO enriched categories
0
5
10
15
Enrichment score

Figure 4

Figure 4. Transcriptomic analysis in roots upon iron deficiency and sufficiency. **(A)** Summary statistics of up- (↑) or down-regulated (↓) genes in different pair-wise comparisons. The direction of comparisons is indicated by arrows. Overlaps in Venn diagrams represent deregulated genes in both Col-0 and *sr45-1* roots in respective comparison (indicated by colors). Right circle: Number of differentially regulated genes solely associated to *sr45-1* roots (SDRs). Left circle: Number of differentially regulated genes solely associated to Col-0. Bar graphs of Gene Ontology (GO) enriched categories in differentially expressed CDR genes **(B)** and SDR genes **(C)**. The enrichment score represents $-\log_{10}(p\text{-value})$. Dissimilar GO terms are colored in red (see also **Supplemental Table 5**).

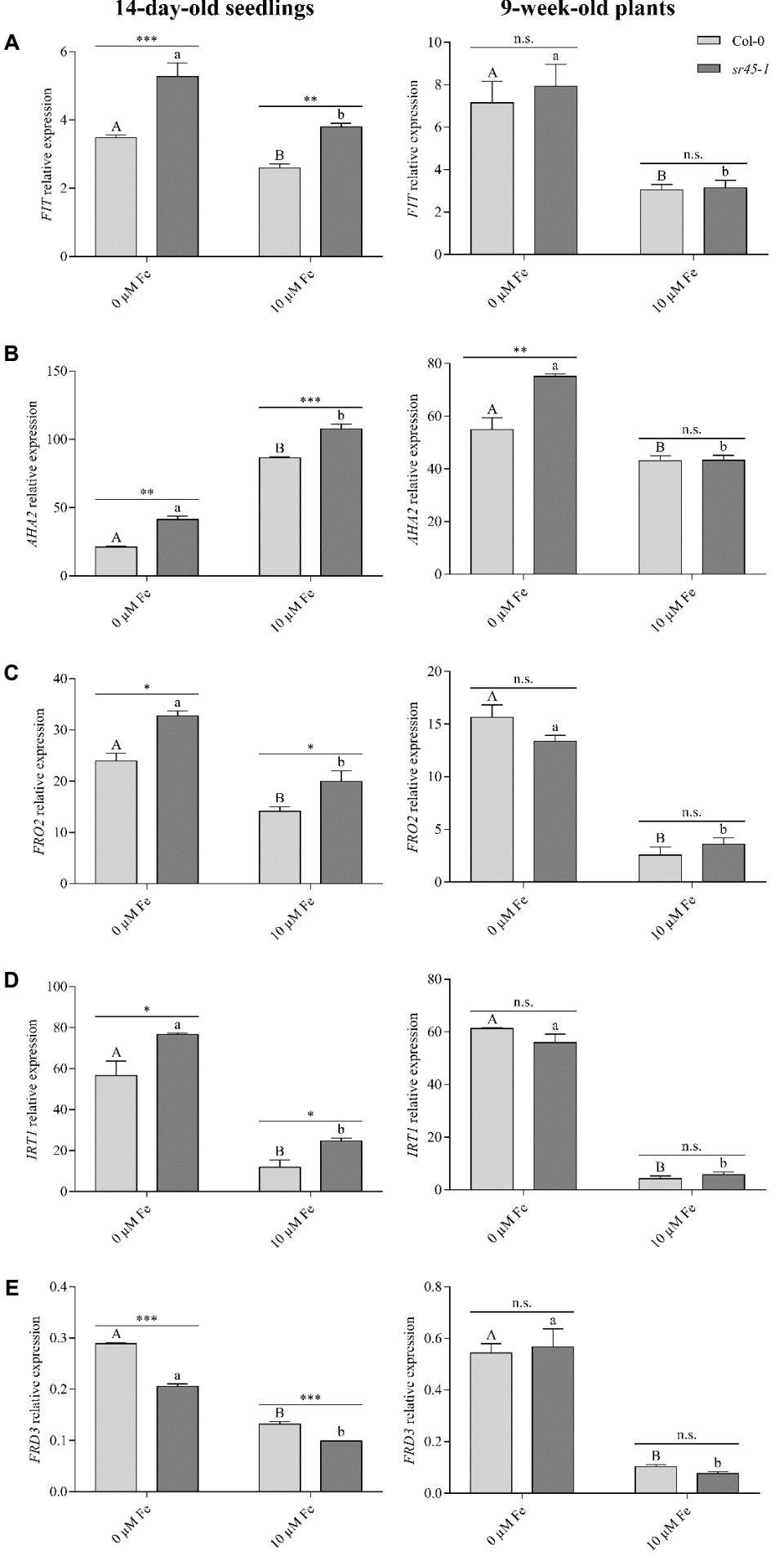
14-day-old seedlings
9-week-old plants
Col-0
sr45-1
A
B
C
D
E
FIT relative expression
AHA2 relative expression
FRO2 relative expression
IRT1 relative expression
FRD3 relative expression
0 µM Fe
10 µM Fe
n.s.

Figure 5

Figure 5. Fe uptake machinery in *sr45-1* seedlings and adult plants. Quantitative RT-PCR analysis of expression of **(A)** *FIT*, **(B)** *AHA2,* **(C)** *FRO2*, **(D)** *IRT1* and **(E)** *FRD3* genes in wild-type (Col-0) and mutant (*sr45-1*) plants grown vertically in petri dishes containing Hoagland medium supplemented with 0 or 10 µM iron (Fe) **(left panel)** and in roots of wild-type (Col-0) and mutant (*sr45-1*) plants grown hydroponically in Hoagland medium supplemented with 0 or 10 µM Fe (RNA-seq samples) **(right panel)**. Values represent means ± SEM (from four biological replicates, each consisting of 2-6 plants per genotype and condition) and are relative to *At1g58050*. Data were analyzed by two-way ANOVA followed by Bonferroni multiple comparison post-test. Statistically significant differences between means between genotypes are indicated by stars (* P<0.05, ** P<0,01, *** P<0.001) or between treatments within genotypes by different letters (P<0.05).

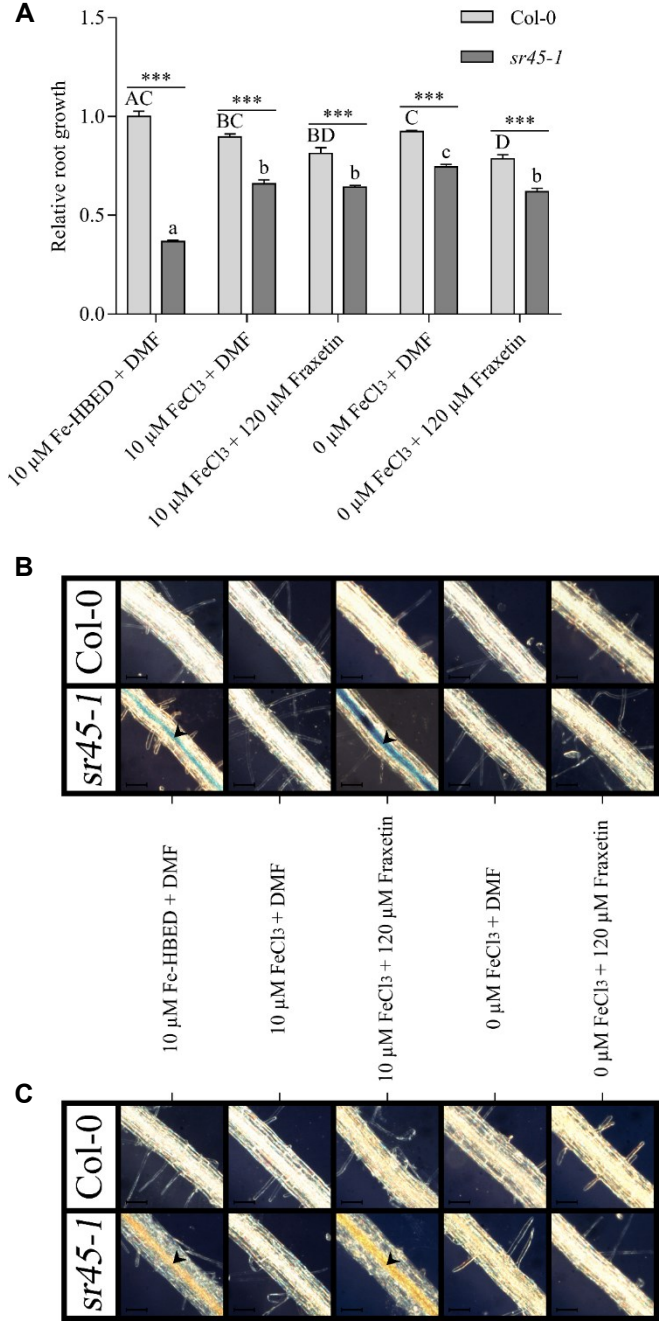
A
Col-0
sr45-1
Relative root growth
1.5
1.0
0.5
0.0
***
AC
a
BC
b
BD
b
C
c
D
b
10 µM Fe-HBED + DMF
10 µM FeCl3 + DMF
10 µM FeCl3 + 120 µM Fraxetin
0 µM FeCl3 + DMF
0 µM FeCl3 + 120 µM Fraxetin
B
Col-0
sr45-1
10 µM Fe-HBED + DMF
10 µM FeCl3 + DMF
10 µM FeCl3 + 120 µM Fraxetin
0 µM FeCl3 + DMF
0 µM FeCl3 + 120 µM Fraxetin
C
Col-0
sr45-1

Figure 6

Figure 6. Effect of exogenous application of coumarins on *sr45-1* roots. **(A)** Relative root growth of wild-type (Col-0) and mutant (*sr45-1*) plants grown vertically in petri dishes containing Hoagland medium supplemented with 10 µM iron (Fe) at various pH (5.7 in presence of Fe-HBED or 7 in presence of $FeCl_3$). Root growth is relative to Col-0 at 10 µM Fe-HBED + DMF (pH 5.7). Values represent means ± SEM (from seven semi-independent experiments, each including 6 plants per genotype and condition). Data were analyzed by two-way ANOVA followed by Bonferroni multiple comparison post-test. Statistically significant differences between means between genotypes are indicated by stars (*** $P<0.001$) or between treatments within genotypes by different letters ($P<0.05$). **(B)** Iron accumulation and **(C)** H_2O_2 accumulation in roots of wild-type (Col-0) and mutant (*sr45-1*) plants grown vertically in petri dishes containing Hoagland medium supplemented with 0 (deficiency) or 10 (control) µM iron (Fe) at various pH (5.7 in presence of Fe-HBED or 7 in presence of $FeCl_3$). The pictures are representative of two semi-independent experiments. Arrowheads show Fe or H_2O_2 accumulation in roots. Scale bar: 100 µm.

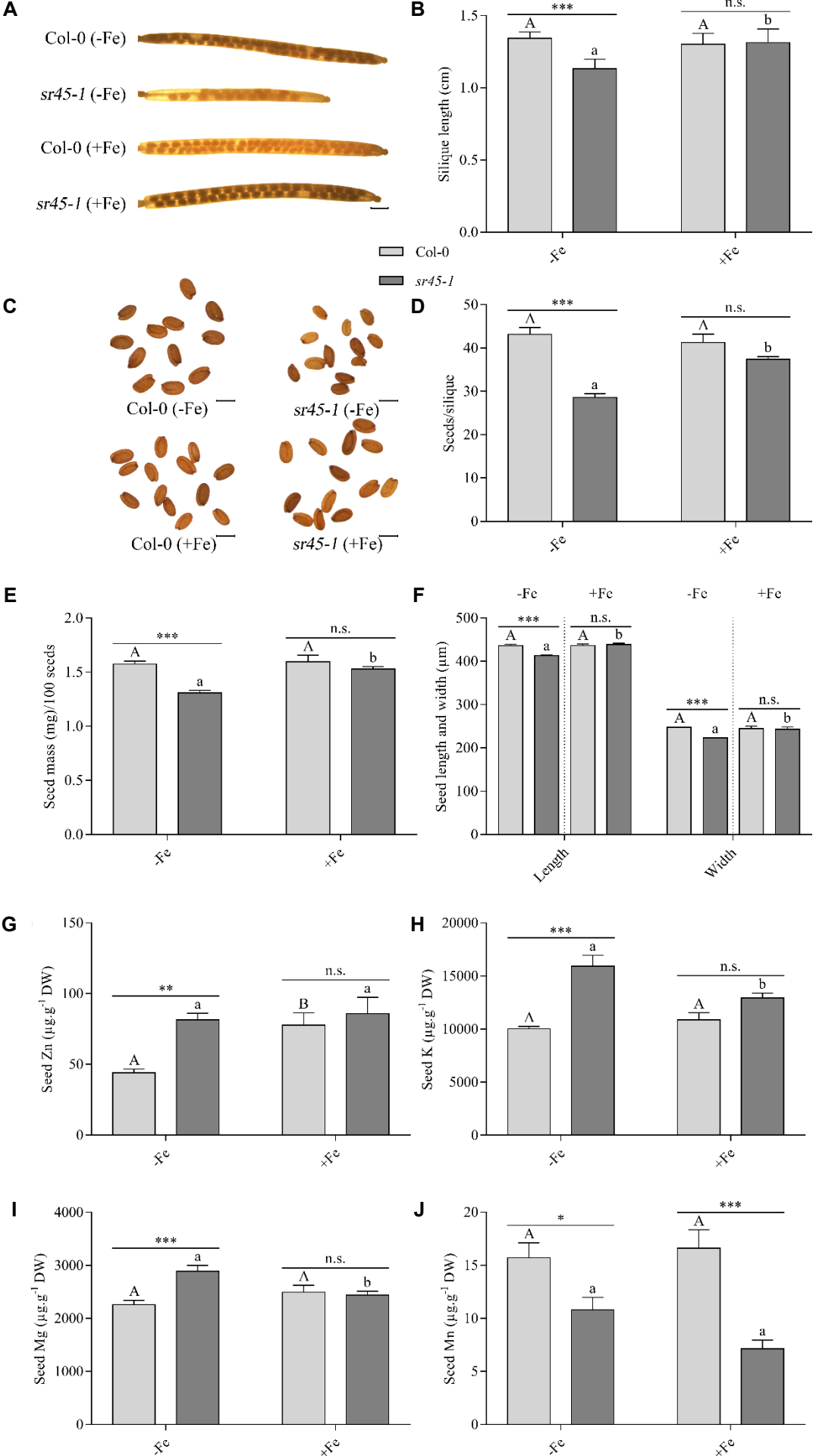
A
Col-0 (-Fe)
sr45-1 (-Fe)
Col-0 (+Fe)
sr45-1 (+Fe)
B
Silique length (cm)
Col-0
sr45-1
-Fe
+Fe
***
n.s.
C
Col-0 (-Fe)
sr45-1 (-Fe)
Col-0 (+Fe)
sr45-1 (+Fe)
D
Seeds/silique
E
Seed mass (mg)/100 seeds
F
Seed length and width (μm)
Length
Width
G
Seed Zn (μg.g-1 DW)
**
H
Seed K (μg.g-1 DW)
I
Seed Mg (μg.g-1 DW)
J
Seed Mn (μg.g-1 DW)
*

Figure 7

Figure 7. Iron irrigation fully rescues the development of the reproductive tissue. **(A)** Representative pictures of wild-type (Col-0) and mutant (*sr45-1*) siliques, **(B)** silique length, **(C)** representative pictures of wild-type (Col-0) and mutant (*sr45-1*) seeds, **(D)** number of seeds per silique, **(E)** seed mass (for pools of 100 seeds), and **(F)** seed length and width of plants grown in soil and daily irrigated with water without (–Fe) or with (+Fe) an additional treatment consisting of a weekly irrigation with sequestrene. Values represent means ± SEM (from three independent experiments with 10-18 siliques pertaining to the main stem [4 plants per genotype and condition] **(B)** or with seeds obtained from 4 plants per genotype and condition **(D-F)**). Scale bars: 1 mm for siliques; 500 µm for seeds. **(G)** Zinc (Zn), **(H)** potassium (K), **(I)** magnesium (Mg) and **(HJ)** manganese (Mn) concentration in seeds (–Fe or +Fe) of wild-type (Col-0) and mutant (*sr45-1*) plants. Values represent means ± SEM (from three independent experiments with seeds obtained from 4 plants per genotype and condition). For each experiment, data were analyzed by two-way ANOVA followed by Bonferroni multiple comparison post-test. Statistically significant differences between means are indicated by stars (* $P<0.05$, ** $P<0,01$, *** $P<0.001$) or different letters ($P<0.05$). **Figure 7F** was obtained by performing statistical analysis for both seed length and seed width independently and then by displaying the results in a single graph.

Parsed Citations

Albaqami, M., Laluk, K., and Reddy, A.S.N. (2019). The Arabidopsis splicing regulator SR45 confers salt tolerance in a splice isoform-dependent manner. Plant Mol Biol 100, 379-390.
Google Scholar: Author Only Title Only Author and Title

Ali, G.S., Palusa, S.G., Golovkin, M., Prasad, J., Manley, J.L., and Reddy, A.S. (2007). Regulation of plant developmental processes by a novel splicing factor. PLoS One 2, e471.
Google Scholar: Author Only Title Only Author and Title

Babst, B.A., Gao, F., Acosta-Gamboa, L.M., Karve, A., Schueller, M.J., and Lorence, A. (2019). Three NPF genes in Arabidopsis are necessary for normal nitrogen cycling under low nitrogen stress. Plant Physiol Biochem 143, 1-10.
Google Scholar: Author Only Title Only Author and Title

Baliardini, C., Meyer, C.L., Salis, P., Saumitou-Laprade, P., and Verbruggen, N. (2015). CATION EXCHANGER1 Cosegregates with Cadmium Tolerance in the Metal Hyperaccumulator Arabidopsis halleri and Plays a Role in Limiting Oxidative Stress in Arabidopsis Spp. Plant Physiol 169, 549-559.
Google Scholar: Author Only Title Only Author and Title

Barberon, M., Vermeer, J.E., De Bellis, D., Wang, P., Naseer, S., Andersen, T.G., Humbel, B.M., Nawrath, C., Takano, J., Salt, D.E., and Geldner, N. (2016). Adaptation of Root Function by Nutrient-Induced Plasticity of Endodermal Differentiation. Cell 164, 447-459.
Google Scholar: Author Only Title Only Author and Title

Barta, A., Kalyna, M., and Reddy, A.S. (2010). Implementing a rational and consistent nomenclature for serine/arginine-rich protein splicing factors (SR proteins) in plants. Plant Cell 22, 2926-2929.
Google Scholar: Author Only Title Only Author and Title

Baxter, I., Hosmani, P.S., Rus, A., Lahner, B., Borevitz, J.O., Muthukumar, B., Mickelbart, M.V., Schreiber, L., Franke, R.B., and Salt, D.E. (2009). Root suberin forms an extracellular barrier that affects water relations and mineral nutrition in Arabidopsis. PLoS Genet 5, e1000492.
Google Scholar: Author Only Title Only Author and Title

Bolger, A.M., Lohse, M., and Usadel, B. (2014). Trimmomatic: a flexible trimmer for Illumina sequence data. Bioinformatics 30, 2114-2120.
Google Scholar: Author Only Title Only Author and Title

Califice, S., Baurain, D., Hanikenne, M., and Motte, P. (2012). A single ancient origin for prototypical serine/arginine-rich splicing factors. Plant Physiol 158, 546-560.
Google Scholar: Author Only Title Only Author and Title

Carvalho, R.F., Carvalho, S.D., and Duque, P. (2010). The plant-specific SR45 protein negatively regulates glucose and ABA signaling during early seedling development in Arabidopsis. Plant Physiol 154, 772-783.
Google Scholar: Author Only Title Only Author and Title

Carvalho, R.F., Szakonyi, D., Simpson, C.G., Barbosa, I.C., Brown, J.W., Baena-González, E., and Duque, P. (2016). The Arabidopsis SR45 Splicing Factor, a Negative Regulator of Sugar Signaling, Modulates SNF1-Related Protein Kinase 1 Stability. Plant Cell 28, 1910-1925.
Google Scholar: Author Only Title Only Author and Title

Castaings, L., Caquot, A., Loubet, S., and Curie, C. (2016). The high-affinity metal Transporters NRAMP1 and IRT1 Team up to Take up Iron under Sufficient Metal Provision. Sci Rep 6, 37222.
Google Scholar: Author Only Title Only Author and Title

Chamala, S., Feng, G., Chavarro, C., and Barbazuk, W.B. (2015). Genome-wide identification of evolutionarily conserved alternative splicing events in flowering plants. Front Bioeng Biotechnol 3, 33.
Google Scholar: Author Only Title Only Author and Title

Charlier, J.B., Polese, C., Nouet, C., Carnol, M., Bosman, B., Krämer, U., Motte, P., and Hanikenne, M. (2015). Zinc triggers a complex transcriptional and post-transcriptional regulation of the metal homeostasis gene FRD3 in Arabidopsis relatives. J Exp Bot 66, 3865-3878.
Google Scholar: Author Only Title Only Author and Title

Chen, S.L., Rooney, T.J., Hu, A.R., Beard, H.S., Garrett, W.M., Mangalath, L.M., Powers, J.J., Cooper, B., and Zhang, X.N. (2019). Quantitative Proteomics Reveals a Role for SERINE/ARGININE-Rich 45 in Regulating RNA Metabolism and Modulating Transcriptional Suppression via the ASAP Complex in Arabidopsis thaliana. Front Plant Sci 10, 1116.
Google Scholar: Author Only Title Only Author and Title

Chen, T., Cui, P., Chen, H., Ali, S., Zhang, S., and Xiong, L. (2013). A KH-domain RNA-binding protein interacts with FIERY2/CTD phosphatase-like 1 and splicing factors and is important for pre-mRNA splicing in Arabidopsis. PLoS Genet 9, e1003875.
Google Scholar: Author Only Title Only Author and Title

Chezem, W.R., Memon, A., Li, F.S., Weng, J.K., and Clay, N.K. (2017). SG2-Type R2R3-MYB Transcription Factor MYB15 Controls Defense-Induced Lignification and Basal Immunity in Arabidopsis. Plant Cell 29, 1907-1926.

Google Scholar: Author Only Title Only Author and Title

Colangelo, E.P., and Guerinot, M.L. (2004). The essential basic helix-loop-helix protein FIT1 is required for the iron deficiency response. Plant Cell 16, 3400-3412.
Google Scholar: Author Only Title Only Author and Title

Cui, Y., Chen, C.L., Cui, M., Zhou, W.J., Wu, H.L., and Ling, H.Q. (2018). Four IVa bHLH Transcription Factors Are Novel Interactors of FIT and Mediate JA Inhibition of Iron Uptake in Arabidopsis. Mol Plant 11, 1166-1183.
Google Scholar: Author Only Title Only Author and Title

Curie, C., and Mari, S. (2017). New routes for plant iron mining. New Phytol 214, 521-525.
Google Scholar: Author Only Title Only Author and Title

Czechowski, T., Stitt, M., Altmann, T., Udvardi, M.K., and Scheible, W.R. (2005). Genome-wide identification and testing of superior reference genes for transcript normalization in Arabidopsis. Plant Physiol 139, 5-17.
Google Scholar: Author Only Title Only Author and Title

Dong, C., He, F., Berkowitz, O., Liu, J., Cao, P., Tang, M., Shi, H., Wang, W., Li, Q., Shen, Z., Whelan, J., and Zheng, L. (2018). Alternative Splicing Plays a Critical Role in Maintaining Mineral Nutrient Homeostasis in Rice (Oryza sativa). Plant Cell 30, 2267-2285.
Google Scholar: Author Only Title Only Author and Title

Dučić, T., and Polle, A. (2007). Manganese toxicity in two varieties of Douglas fir (Pseudotsuga menziesii var. viridis and glauca) seedlings as affected by phosphorus supply. Functional Plant Biology 34, 31-40.
Google Scholar: Author Only Title Only Author and Title

Durrett, T.P., Gassmann, W., and Rogers, E.E. (2007). The FRD3-mediated efflux of citrate into the root vasculature is necessary for efficient iron translocation. Plant Physiol 144, 197-205.
Google Scholar: Author Only Title Only Author and Title

El-Ashgar, N.M., El-Basioni, A., El-Nahhal, I.M., Zourob, S.M., El-Agez, T.M., and Taya, S.A. (2012). Sol-Gel Thin Films Immobilized with Bromocresol Purple pH-Sensitive Indicator in Presence of Surfactants. ISRN Analytical Chemistry 2012.
Google Scholar: Author Only Title Only Author and Title

Fan, S.C., Lin, C.S., Hsu, P.K., Lin, S.H., and Tsay, Y.F. (2009). The Arabidopsis nitrate transporter NRT1.7, expressed in phloem, is responsible for source-to-sink remobilization of nitrate. Plant Cell 21, 2750-2761.
Google Scholar: Author Only Title Only Author and Title

Fourcroy, P., Sisó-Terraza, P., Sudre, D., Saviron, M., Reyt, G., Gaymard, F., Abadía, A., Abadia, J., Álvarez-Fernández, A., and Briat, J.F. (2014). Involvement of the ABCG37 transporter in secretion of scopoletin and derivatives by Arabidopsis roots in response to iron deficiency. New Phytol 201, 155-167.
Google Scholar: Author Only Title Only Author and Title

Fukao, Y., Ferjani, A., Tomioka, R., Nagasaki, N., Kurata, R., Nishimori, Y., Fujiwara, M., and Maeshima, M. (2011). iTRAQ analysis reveals mechanisms of growth defects due to excess zinc in Arabidopsis. Plant Physiol 155, 1893-1907.
Google Scholar: Author Only Title Only Author and Title

García, M.J., Lucena, C., Romera, F.J., Alcántara, E., and Pérez-Vicente, R. (2010). Ethylene and nitric oxide involvement in the up-regulation of key genes related to iron acquisition and homeostasis in Arabidopsis. J Exp Bot 61, 3885-3899.
Google Scholar: Author Only Title Only Author and Title

Geldner, N. (2013). The endodermis. Annu Rev Plant Biol 64, 531-558.
Google Scholar: Author Only Title Only Author and Title

Glaring, M.A., Zygadlo, A., Thorneycroft, D., Schulz, A., Smith, S.M., Blennow, A., and Baunsgaard, L. (2007). An extra-plastidial alpha-glucan, water dikinase from Arabidopsis phosphorylates amylopectin in vitro and is not necessary for transient starch degradation. J Exp Bot 58, 3949-3960.
Google Scholar: Author Only Title Only Author and Title

Golovkin, M., and Reddy, A.S. (1999). An SC35-like protein and a novel serine/arginine-rich protein interact with Arabidopsis U1-70K protein. J Biol Chem 274, 36428-36438.
Google Scholar: Author Only Title Only Author and Title

Green, L.S., and Rogers, E.E. (2004). FRD3 controls iron localization in Arabidopsis. Plant Physiol 136, 2523-2531.
Google Scholar: Author Only Title Only Author and Title

Guo, W., Nazim, H., Liang, Z., and Yang, D. (2016). Magnesium deficiency in plants: An urgent problem. The Crop Journal 4, 83-91.
Google Scholar: Author Only Title Only Author and Title

Hanikenne, M., Esteves, S.M., Fanara, S., and Rouached, H. (2021). Coordinated homeostasis of essential mineral nutrients: a focus on iron. J Exp Bot 72, 2136-2153.
Google Scholar: Author Only Title Only Author and Title

Hanikenne, M., Talke, I.N., Haydon, M.J., Lanz, C., Nolte, A., Motte, P., Kroymann, J., Weigel, D., and Krämer, U. (2008). Evolution of metal hyperaccumulation required cis-regulatory changes and triplication of HMA4. Nature 453, 391-395.

Google Scholar: Author Only Title Only Author and Title

Haydon, M.J., Kawachi, M., Wirtz, M., Hillmer, S., Hell, R., and Krämer, U. (2012). Vacuolar nicotianamine has critical and distinct roles under iron deficiency and for zinc sequestration in Arabidopsis. Plant Cell 24, 724-737.
Google Scholar: Author Only Title Only Author and Title

Hindt, M.N., Akmakjian, G.Z., Pivarski, K.L., Punshon, T., Baxter, I., Salt, D.E., and Guerinot, M.L. (2017). BRUTUS and its paralogs, BTS LIKE1 and BTS LIKE2, encode important negative regulators of the iron deficiency response in Arabidopsis thaliana. Metallomics 9, 876-890.
Google Scholar: Author Only Title Only Author and Title

Ivanov, R., Brumbarova, T., and Bauer, P. (2012). Fitting into the harsh reality: regulation of iron-deficiency responses in dicotyledonous plants. Mol Plant 5, 27-42.
Google Scholar: Author Only Title Only Author and Title

Jakoby, M., Wang, H.Y., Reidt, W., Weisshaar, B., and Bauer, P. (2004). FRU (BHLH029) is required for induction of iron mobilization genes in Arabidopsis thaliana. FEBS Lett 577, 528-534.
Google Scholar: Author Only Title Only Author and Title

Jeong, S. (2017). SR Proteins: Binders, Regulators, and Connectors of RNA. Mol Cells 40, 1-9.
Google Scholar: Author Only Title Only Author and Title

Kailasam, S., Wang, Y., Lo, J.C., Chang, H.F., and Yeh, K.C. (2018). S-Nitrosoglutathione works downstream of nitric oxide to mediate iron-deficiency signaling in Arabidopsis. Plant J 94, 157-168.
Google Scholar: Author Only Title Only Author and Title

Kamiya, T., Borghi, M., Wang, P., Danku, J.M., Kalmbach, L., Hosmani, P.S., Naseer, S., Fujiwara, T., Geldner, N., and Salt, D.E. (2015). The MYB36 transcription factor orchestrates Casparian strip formation. Proc Natl Acad Sci U S A 112, 10533-10538.
Google Scholar: Author Only Title Only Author and Title

Kawachi, M., Kobae, Y., Mori, H., Tomioka, R., Lee, Y., and Maeshima, M. (2009). A mutant strain Arabidopsis thaliana that lacks vacuolar membrane zinc transporter MTP1 revealed the latent tolerance to excessive zinc. Plant Cell Physiol 50, 1156-1170.
Google Scholar: Author Only Title Only Author and Title

Kobayashi, T., Nagasaka, S., Senoura, T., Itai, R.N., Nakanishi, H., and Nishizawa, N.K. (2013). Iron-binding haemerythrin RING ubiquitin ligases regulate plant iron responses and accumulation. Nat Commun 4, 2792.
Google Scholar: Author Only Title Only Author and Title

Laloum, T., Martín, G., and Duque, P. (2018). Alternative Splicing Control of Abiotic Stress Responses. Trends Plant Sci 23, 140-150.
Google Scholar: Author Only Title Only Author and Title

Le, C.T., Brumbarova, T., Ivanov, R., Stoof, C., Weber, E., Mohrbacher, J., Fink-Straube, C., and Bauer, P. (2016). ZINC FINGER OF ARABIDOPSIS THALIANA12 (ZAT12) Interacts with FER-LIKE IRON DEFICIENCY-INDUCED TRANSCRIPTION FACTOR (FIT) Linking Iron Deficiency and Oxidative Stress Responses. Plant Physiol 170, 540-557.
Google Scholar: Author Only Title Only Author and Title

Lei, Y., Korpelainen, H., and Li, C. (2007). Physiological and biochemical responses to high Mn concentrations in two contrasting Populus cathayana populations. Chemosphere 68, 686-694.
Google Scholar: Author Only Title Only Author and Title

Li, J., Zhang, M., Sun, J., Mao, X., Wang, J., Liu, H., Zheng, H., Li, X., Zhao, H., and Zou, D. (2020). Heavy Metal Stress-Associated Proteins in Rice and Arabidopsis: Genome-Wide Identification, Phylogenetics, Duplication, and Expression Profiles Analysis. Front Genet 11, 477.
Google Scholar: Author Only Title Only Author and Title

Lichtenthaler, H.K., and Buschmann, C. (2001). Chlorophylls and Carotenoids: Measurement and Characterization by UV-VIS Spectroscopy. Current Protocols in Food Analytical Chemistry F4, 1– F4.3.8.
Google Scholar: Author Only Title Only Author and Title

Lingam, S., Mohrbacher, J., Brumbarova, T., Potuschak, T., Fink-Straube, C., Blondet, E., Genschik, P., and Bauer, P. (2011). Interaction between the bHLH transcription factor FIT and ETHYLENE INSENSITIVE3/ETHYLENE INSENSITIVE3-LIKE1 reveals molecular linkage between the regulation of iron acquisition and ethylene signaling in Arabidopsis. Plant Cell 23, 1815-1829.
Google Scholar: Author Only Title Only Author and Title

Liu, M., Liu, X.X., He, X.L., Liu, L.J., Wu, H., Tang, C.X., Zhang, Y.S., and Jin, C.W. (2017a). Ethylene and nitric oxide interact to regulate the magnesium deficiency-induced root hair development in Arabidopsis. New Phytol 213, 1242-1256.
Google Scholar: Author Only Title Only Author and Title

Liu, M., Zhang, H., Fang, X., Zhang, Y., and Jin, C. (2018). Auxin Acts Downstream of Ethylene and Nitric Oxide to Regulate Magnesium Deficiency-Induced Root Hair Development in Arabidopsis thaliana. Plant Cell Physiol 59, 1452-1465.
Google Scholar: Author Only Title Only Author and Title

Liu, W., Sun, Q., Wang, K., Du, Q., and Li, W.X. (2017b). Nitrogen Limitation Adaptation (NLA) is involved in source-to-sink remobilization of nitrate by mediating the degradation of NRT1.7 in Arabidopsis. New Phytol 214, 734-744.

Google Scholar: Author Only Title Only Author and Title

Long, T.A., Tsukagoshi, H., Busch, W., Lahner, B., Salt, D.E., and Benfey, P.N. (2010). The bHLH transcription factor POPEYE regulates response to iron deficiency in Arabidopsis roots. Plant Cell 22, 2219-2236.
Google Scholar: Author Only Title Only Author and Title

Love, M.I., Huber, W., and Anders, S. (2014). Moderated estimation of fold change and dispersion for RNA-seq data with DESeq2. Genome Biology 15, 550.
Google Scholar: Author Only Title Only Author and Title

Manley, J.L., and Krainer, A.R. (2010). A rational nomenclature for serine/arginine-rich protein splicing factors (SR proteins). Genes Dev 24, 1073-1074.
Google Scholar: Author Only Title Only Author and Title

Marschner, H., and Marschner, P. (2012). Marschner's Mineral Nutrition of Higher Plants (3rd edition). Academic Press.
Google Scholar: Author Only Title Only Author and Title

Meyer, K., Koester, T., and Staiger, D. (2015). Pre-mRNA Splicing in Plants: In Vivo Functions of RNA-Binding Proteins Implicated in the Splicing Process. Biomolecules 5, 1717-1740.
Google Scholar: Author Only Title Only Author and Title

Millaleo, R., Reyes-Díaz, M., Alberdi, M., Ivanov, A.G., Krol, M., and Hüner, N.P. (2013). Excess manganese differentially inhibits photosystem I versus II in Arabidopsis thaliana. J Exp Bot 64, 343-354.
Google Scholar: Author Only Title Only Author and Title

Mladenka, P., Macáková, K., Zatloukalová, L., Reháková, Z., Singh, B.K., Prasad, A.K., Parmar, V.S., Jahodár, L., Hrdina, R., and Saso, L. (2010). In vitro interactions of coumarins with iron. Biochimie 92, 1108-1114.
Google Scholar: Author Only Title Only Author and Title

Morrissey, J., Baxter, I.R., Lee, J., Li, L., Lahner, B., Grotz, N., Kaplan, J., Salt, D.E., and Guerinot, M.L. (2009). The ferroportin metal efflux proteins function in iron and cobalt homeostasis in Arabidopsis. Plant Cell 21, 3326-3338.
Google Scholar: Author Only Title Only Author and Title

Nouet, C., Charlier, J.B., Carnol, M., Bosman, B., Farnir, F., Motte, P., and Hanikenne, M. (2015). Functional analysis of the three HMA4 copies of the metal hyperaccumulator Arabidopsis halleri. J Exp Bot 66, 5783-5795.
Google Scholar: Author Only Title Only Author and Title

Nouet, C., Motte, P., and Hanikenne, M. (2011). Chloroplastic and mitochondrial metal homeostasis. Trends Plant Sci 16, 395-404.
Google Scholar: Author Only Title Only Author and Title

Palmer, C.M., Hindt, M.N., Schmidt, H., Clemens, S., and Guerinot, M.L. (2013). MYB10 and MYB72 are required for growth under iron-limiting conditions. PLoS Genet 9, e1003953.
Google Scholar: Author Only Title Only Author and Title

Palusa, S.G., Ali, G.S., and Reddy, A.S. (2007). Alternative splicing of pre-mRNAs of Arabidopsis serine/arginine-rich proteins: regulation by hormones and stresses. Plant J 49, 1091-1107.
Google Scholar: Author Only Title Only Author and Title

Palusa, S.G., and Reddy, A.S. (2010). Extensive coupling of alternative splicing of pre-mRNAs of serine/arginine (SR) genes with nonsense-mediated decay. New Phytol 185, 83-89.
Google Scholar: Author Only Title Only Author and Title

Petridis, A., Döll, S., Nichelmann, L., Bilger, W., and Mock, H.P. (2016). Arabidopsis thaliana G2-LIKE FLAVONOID REGULATOR and BRASSINOSTEROID ENHANCED EXPRESSION1 are low-temperature regulators of flavonoid accumulation. New Phytol 211, 912-925.
Google Scholar: Author Only Title Only Author and Title

Pfaffl, M.W. (2001). A new mathematical model for relative quantification in real-time RT-PCR. Nucleic Acids Res 29, e45.
Google Scholar: Author Only Title Only Author and Title

Pirone, C., Gurrieri, L., Gaiba, I., Adamiano, A., Valle, F., Trost, P., and Sparla, F. (2017). The analysis of the different functions of starch-phosphorylating enzymes during the development of Arabidopsis thaliana plants discloses an unexpected role for the cytosolic isoform GWD2. Physiol Plant 160, 447-457.
Google Scholar: Author Only Title Only Author and Title

Rajniak, J., Giehl, R.F.H., Chang, E., Murgia, I., von Wirén, N., and Sattely, E.S. (2018). Biosynthesis of redox-active metabolites in response to iron deficiency in plants. Nat Chem Biol 14, 442-450.
Google Scholar: Author Only Title Only Author and Title

Ravet, K., Touraine, B., Boucherez, J., Briat, J.F., Gaymard, F., and Cellier, F. (2009). Ferritins control interaction between iron homeostasis and oxidative stress in Arabidopsis. Plant J 57, 400-412.
Google Scholar: Author Only Title Only Author and Title

Remy, E., Cabrito, T.R., Batista, R.A., Hussein, M.A., Teixeira, M.C., Athanasiadis, A., Sá-Correia, I., and Duque, P. (2014). Intron retention in the 5'UTR of the novel ZIF2 transporter enhances translation to promote zinc tolerance in Arabidopsis. PLoS Genet 10,

e1004375.
Google Scholar: Author Only Title Only Author and Title

Reyt, G., Boudouf, S., Boucherez, J., Gaymard, F., and Briat, J.F. (2015). Iron- and ferritin-dependent reactive oxygen species distribution: impact on Arabidopsis root system architecture. Mol Plant 8, 439-453.
Google Scholar: Author Only Title Only Author and Title

Robinson, N.J., Procter, C.M., Connolly, E.L., and Guerinot, M.L. (1999). A ferric-chelate reductase for iron uptake from soils. Nature 397, 694-697.
Google Scholar: Author Only Title Only Author and Title

Rodríguez-Celma, J., Connorton, J.M., Kruse, I., Green, R.T., Franceschetti, M., Chen, Y.T., Cui, Y., Ling, H.Q., Yeh, K.C., and Balk, J. (2019). Arabidopsis BRUTUS-LIKE E3 ligases negatively regulate iron uptake by targeting transcription factor FIT for recycling. Proc Natl Acad Sci U S A 116, 17584-17591.
Google Scholar: Author Only Title Only Author and Title

Römheld, V., and Marschner, H. (1986). Evidence for a specific uptake system for iron phytosiderophores in roots of grasses. Plant Physiol 80, 175-180.
Google Scholar: Author Only Title Only Author and Title

Roschzttardtz, H., Conéjéro, G., Curie, C., and Mari, S. (2009). Identification of the endodermal vacuole as the iron storage compartment in the Arabidopsis embryo. Plant Physiol 151, 1329-1338.
Google Scholar: Author Only Title Only Author and Title

Roschzttardtz, H., Seguela-Arnaud, M., Briat, J.F., Vert, G., and Curie, C. (2011). The FRD3 citrate effluxer promotes iron nutrition between symplastically disconnected tissues throughout Arabidopsis development. Plant Cell 23, 2725-2737.
Google Scholar: Author Only Title Only Author and Title

Santi, S., and Schmidt, W. (2009). Dissecting iron deficiency-induced proton extrusion in Arabidopsis roots. New Phytol 183, 1072-1084.
Google Scholar: Author Only Title Only Author and Title

Scheepers, M., Spielmann, J., Boulanger, M., Carnol, M., Bosman, B., De Pauw, E., Goormaghtigh, E., Motte, P., and Hanikenne, M. (2020). Intertwined metal homeostasis, oxidative and biotic stress responses in the Arabidopsis frd3 mutant. Plant J.
Google Scholar: Author Only Title Only Author and Title

Schmidt, H., Günther, C., Weber, M., Spörlein, C., Loscher, S., Böttcher, C., Schobert, R., and Clemens, S. (2014). Metabolome analysis of Arabidopsis thaliana roots identifies a key metabolic pathway for iron acquisition. PLoS One 9, e102444.
Google Scholar: Author Only Title Only Author and Title

Schvartzman, M.S., Corso, M., Fataftah, N., Scheepers, M., Nouet, C., Bosman, B., Carnol, M., Motte, P., Verbruggen, N., and Hanikenne, M. (2018). Adaptation to high zinc depends on distinct mechanisms in metallicolous populations of Arabidopsis halleri. New Phytol 218, 269-282.
Google Scholar: Author Only Title Only Author and Title

Selote, D., Samira, R., Matthiadis, A., Gillikin, J.W., and Long, T.A. (2015). Iron-binding E3 ligase mediates iron response in plants by targeting basic helix-loop-helix transcription factors. Plant Physiol 167, 273-286.
Google Scholar: Author Only Title Only Author and Title

Shang, X., Cao, Y., and Ma, L. (2017). Alternative Splicing in Plant Genes: A Means of Regulating the Environmental Fitness of Plants. Int J Mol Sci 18.
Google Scholar: Author Only Title Only Author and Title

Shanmugam, V., Lo, J.C., Wu, C.L., Wang, S.L., Lai, C.C., Connolly, E.L., Huang, J.L., and Yeh, K.C. (2011). Differential expression and regulation of iron-regulated metal transporters in Arabidopsis halleri and Arabidopsis thaliana - the role in zinc tolerance. New Phytol 190, 125-137.
Google Scholar: Author Only Title Only Author and Title

Singh, S.K., and Reddy, V.R. (2017). Potassium Starvation Limits Soybean Growth More than the Photosynthetic Processes across CO2 Levels. Front Plant Sci 8, 991.
Google Scholar: Author Only Title Only Author and Title

Sivitz, A.B., Hermand, V., Curie, C., and Vert, G. (2012). Arabidopsis bHLH100 and bHLH101 control iron homeostasis via a FIT-independent pathway. PLoS One 7, e44843.
Google Scholar: Author Only Title Only Author and Title

Siwinska, J., Siatkowska, K., Olry, A., Grosjean, J., Hehn, A., Bourgaud, F., Meharg, A.A., Carey, M., Lojkowska, E., and Ihnatowicz, A. (2018). Scopoletin 8-hydroxylase: a novel enzyme involved in coumarin biosynthesis and iron-deficiency responses in Arabidopsis. J Exp Bot 69, 1735-1748.
Google Scholar: Author Only Title Only Author and Title

Song, W.Y., Choi, K.S., Kim, D.Y., Geisler, M., Park, J., Vincenzetti, V., Schellenberg, M., Kim, S.H., Lim, Y.P., Noh, E.W., Lee, Y., and Martinoia, E. (2010). Arabidopsis PCR2 is a zinc exporter involved in both zinc extrusion and long-distance zinc transport. Plant Cell 22, 2237-2252.

Google Scholar: Author Only Title Only Author and Title

Spielmann, J., Ahmadi, H., Scheepers, M., Weber, M., Nitsche, S., Carnol, M., Bosman, B., Kroymann, J., Motte, P., Clemens, S., and Hanikenne, M. (2020). The two copies of the zinc and cadmium ZIP6 transporter of Arabidopsis halleri have distinct effects on cadmium tolerance. Plant Cell Environ 43, 2143-2157.
Google Scholar: Author Only Title Only Author and Title

Stacey, M.G., Patel, A., McClain, W.E., Mathieu, M., Remley, M., Rogers, E.E., Gassmann, W., Blevins, D.G., and Stacey, G. (2008). The Arabidopsis AtOPT3 protein functions in metal homeostasis and movement of iron to developing seeds. Plant Physiol 146, 589-601.
Google Scholar: Author Only Title Only Author and Title

Talke, I.N., Hanikenne, M., and Krämer, U. (2006). Zinc-dependent global transcriptional control, transcriptional deregulation, and higher gene copy number for genes in metal homeostasis of the hyperaccumulator Arabidopsis halleri. Plant Physiol 142, 148-167.
Google Scholar: Author Only Title Only Author and Title

Tehseen, M., Cairns, N., Sherson, S., and Cobbett, C.S. (2010). Metallochaperone-like genes in Arabidopsis thaliana. Metallomics 2, 556-564.
Google Scholar: Author Only Title Only Author and Title

Thomine, S., and Vert, G. (2013). Iron transport in plants: better be safe than sorry. Curr Opin Plant Biol 16, 322-327.
Google Scholar: Author Only Title Only Author and Title

Tsai, H.H., Rodríguez-Celma, J., Lan, P., Wu, Y.C., Vélez-Bermúdez, I.C., and Schmidt, W. (2018). Scopoletin 8-Hydroxylase-Mediated Fraxetin Production Is Crucial for Iron Mobilization. Plant Physiol 177, 194-207.
Google Scholar: Author Only Title Only Author and Title

Verbruggen, N., and Hermans, C. (2013). Physiological and molecular responses to magnesium nutritional imbalance in plants. Plant and Soil 368, 87-99.
Google Scholar: Author Only Title Only Author and Title

Vert, G., Grotz, N., Dédaldéchamp, F., Gaymard, F., Guerinot, M.L., Briat, J.F., and Curie, C. (2002). IRT1, an Arabidopsis transporter essential for iron uptake from the soil and for plant growth. Plant Cell 14, 1223-1233.
Google Scholar: Author Only Title Only Author and Title

Wang, N., Cui, Y., Liu, Y., Fan, H., Du, J., Huang, Z., Yuan, Y., Wu, H., and Ling, H.Q. (2013). Requirement and functional redundancy of Ib subgroup bHLH proteins for iron deficiency responses and uptake in Arabidopsis thaliana. Mol Plant 6, 503-513.
Google Scholar: Author Only Title Only Author and Title

Wintermans, J.F., and de Mots, A. (1965). Spectrophotometric characteristics of chlorophylls a and b and their pheophytins in ethanol. Biochim Biophys Acta 109, 448-453.
Google Scholar: Author Only Title Only Author and Title

Xing, D., Wang, Y., Hamilton, M., Ben-Hur, A., and Reddy, A.S. (2015). Transcriptome-Wide Identification of RNA Targets of Arabidopsis SERINE/ARGININE-RICH45 Uncovers the Unexpected Roles of This RNA Binding Protein in RNA Processing. Plant Cell 27, 3294-3308.
Google Scholar: Author Only Title Only Author and Title

Yi, Y., and Guerinot, M.L. (1996). Genetic evidence that induction of root Fe(III) chelate reductase activity is necessary for iron uptake under iron deficiency. Plant J 10, 835-844.
Google Scholar: Author Only Title Only Author and Title

Yuan, Y., Wu, H., Wang, N., Li, J., Zhao, W., Du, J., Wang, D., and Ling, H.Q. (2008). FIT interacts with AtbHLH38 and AtbHLH39 in regulating iron uptake gene expression for iron homeostasis in Arabidopsis. Cell Res 18, 385-397.
Google Scholar: Author Only Title Only Author and Title

Zhang, W., Du, B., Liu, D., and Qi, X. (2014). Splicing factor SR34b mutation reduces cadmium tolerance in Arabidopsis by regulating iron-regulated transporter 1 gene. Biochem Biophys Res Commun 455, 312-317.
Google Scholar: Author Only Title Only Author and Title

Zhang, X.N., and Mount, S.M. (2009). Two alternatively spliced isoforms of the Arabidopsis SR45 protein have distinct roles during normal plant development. Plant Physiol 150, 1450-1458.
Google Scholar: Author Only Title Only Author and Title

Zhang, X.N., Shi, Y., Powers, J.J., Gowda, N.B., Zhang, C., Ibrahim, H.M.M., Ball, H.B., Chen, S.L., Lu, H., and Mount, S.M. (2017). Transcriptome analyses reveal SR45 to be a neutral splicing regulator and a suppressor of innate immunity in Arabidopsis thaliana. BMC Genomics 18, 772.
Google Scholar: Author Only Title Only Author and Title